Materials Research Express

PAPER • OPEN ACCESS

Electrospinning process parameters optimization for biofunctional curcumin/gelatin nanofibers

To cite this article: Nand Jee Kanu *et al* 2020 *Mater. Res. Express* **7** 035022

Materials Research Express

OPEN ACCESS

RECEIVED
11 January 2020

REVISED
5 March 2020

ACCEPTED FOR PUBLICATION
12 March 2020

PUBLISHED
23 March 2020

PAPER

Electrospinning process parameters optimization for biofunctional curcumin/gelatin nanofibers

Nand Jee Kanu[1,4], **Eva Gupta**[2], **Umesh Kumar Vates**[2] and **Gyanendra Kumar Singh**[3]

[1] S. V. National Institute of Technology, Surat, India
[2] Amity University, Uttar Pradesh, India
[3] Faculty, Adama Science and Technology University, Adama, Ethiopia
[4] Author to whom any correspondence should be addressed.

E-mail: nandssm@gmail.com, evagupta695@gmail.com, ukvates@amity.edu and gksinghits@yahoo.co.in

Keywords: Electrospinning, nanofibers, curcumin, gelatin

Abstract

Electrospinning has received wide attention for the preparation of uniform diameter nanofibers (ranging from 5 nm to several hundred nanometers) in films with random as well as aligned fashions of the fibers of various materials for use in biomedical applications. Electrospinning research has provided an in-depth understanding of the preparation of light weight, ultrathin, porous, biofunctional curcumin/gelatin nanofibers having applications in wound dressing, drug release, tissue engineering, etc. In the first half of this article, prior research on electrospun curcumin/gelatin nanofibers is reviewed in depth with nanofibers being desired due to their low diameters since these would have then large surface area to volume ratio and enough film porosity as well as improved mechanical (tensile) strength so that when prepared as mats these nanofibers (having high biocompatibility) could be used for sustained release of curcumin and oxygen to wounds during healing. The synthesis of ultrathin nanofibers (having minimum average diameter) is not a simple task unless numerical investigation is carefully done in the first half of this research article. The authors research described here examined the effects of critical process parameters (in the second half of the paper) such as distance between the spinneret and collector, flow rate, voltage and solution viscosity, on the preparation of uniform and ultrathin nanofibers using scanning electron microscopy (SEM) for characterization of the nanofibers. A 2^k factorial design of experiment was found to be a suitable and efficient technique to optimize the critical process parameters used in the preparation of the biofunctional nanofibers with the purpose of having applications in the treatment of problematic wounds such as diabetic chronic ulcers. After parametric investigation, the distance, flow rate and voltage when taken together, were found to have the most significant contributions to the preparation of minimum diameter nanofibers. The primary objective of this research was fulfilled with the development of ultrathin curcumin/gelatin nanofibers having a 181 nm (181 $\pm$ 66 nm) average diameter using the optimized setting of a solution having 1.5% gelatin, and 1% curcumin in 10 ml of 98% concentrated formic acid, with the electrospining unit having a voltage of 10 KV, distance from the spinneret to collector drum of 15 cm, flow rate of 0.1 ml h^{-1}, viscosity of 65 cP and drum collector speed of 1000 rpm. However, the lowest average diameter of nanofiber was measured around 147 nm (147 $\pm$ 34 nm) which was prepared at a higher voltage, such as 15 KV (at 10 cm distance, 0.15 ml h^{-1} flow rate and 65 cP viscosity) using the solution. The design of this research paper is based on the view that merely optimization of biofunctional nanofibers may not fully satisfy researchers/engineers unless they are also provided with sufficient information about (a) the entire electrospinning mechanism (numerical investigations of the mechanism) to have better control over preparation of ultrathin nanofibers, and (b) applications of the resulting ultrathin biofunctional nanofibers while fabricating nanofibrous mats (as used now-a-days) for sustained release of curcumin during the critical hours of wound healing and other biomedical applications.

1. Introduction

1.1. Electrospun curcumin/gelatin nanofibers: review of the state-of-the-art

The impact of nanotechnology on health sciences is widespread. The potential roles of nanofibers in biomedical applications, such as drug release and tissue engineering have been investigated recently. Preparation of polymeric fibers is not a simple task. There are many preparation processes possible which can vary the characteristics of polymeric fibers of the available techniques, electrospinning is considered as an efficient technique to prepare polymeric nanofibers that are polymeric, synthetic or natural, biodegradable or non-biodegradable, etc, having uniform diameters (5 nm to several hundred nanometers) from a wide variety of polymers and composite solutions [1–3]. Electrospinning is preferred over other conventional methods in recent research papers to prepare polymer nanofibers. The apparatus is relatively easy to operate which makes this process cost effective [4–6]. The nanofibers produced so far have applications in many disciplines of engineering and medical sciences. The basics of nanofiber spinning of biopolymers have been described by Jamil *et al* [7]; Pham *et al* [8]; Vasita and katti *et al* [9]; Kriegel *et al* [10]; Shekh *et al* [11]; Tuerdimaimaiti *et al* [12]; Amariei *et al* [13]; Yoon *et al* [14]; Alharbi *et al* [15]; Chen *et al* [16].

The proteins and their derivatives as well as biodegradable and nontoxic biopolymers such as chitosan, cellulose, collagen, gelatin, etc, are extracted from living organisms and they are used for electrospinning of polymeric nanofibers. The limitations of biopolymers such as their limited solubility in organic solvents due to their high crystallinity, their expensive purification processes and further their viscous solutions due to their tendency to form hydrogen bonds, are overcome after blending with synthetic polymers otherwise these limitations may restrict their electrospinning into nanofibrous mats [10]. The nanofibrous mats prepared from electrospun collagen nanofibers have been used as scaffolds for tissue engineering applications [7]. Aloe vera, a natural polymer also holds potential for tissue engineering applications due to its antioxidant and nontoxic nature [11]. The biomedical applications of few electrospun nanofibers are listed in table 1.

Gelatin (a mixture of proteins and peptides) is a natural polymer which is biocompatible, nontoxic and biodegradable, and hence is considered as a fair and safe choice when selecting fiber material for dressing problematic wounds such as diabetic chronic ulcers. The light weight ultrathin nanofibers can serve as mechanical support during wound dressings due to their significant tensile strength as compared to conventional fibers (having diameters in the range of over 100 nm) and also act as barriers to cover the wound [30–33]. Gelatin is also known for its excellent water absorption and fluid affinity, which makes it a good choice to support moist wound healing. Gelatin (a natural biopolymer which is a denatured form of collagen) is quite soluble in formic acid. Collagen is a protein available in the extra cellular matrix (ECM) of animals and humans, and is expensive due to its manufacturing processes. However, gelatin is easily available at a much lower price than collagen and thus is a preferred source for biomaterials. Gelatin nanofibers (like collagen) have been used in biomedical applications such as cosmetics, wound dressing, tissue engineering, surgical treatments, etc [34]. Gelatin nanofibers (having sufficient mechanical properties to be used in these applications as nanofibrous mats) have been electrospun for ultrathin nanofibers [34–44]. These authors also reported that the properties of these nanofibers can be tailored as per requirements by optimizing input parameters such as voltage, viscosity, distance between the spinneret and rotating drum collector, and flow rate. These authors have spun nanofibers of diameters in the range of 76–100 nm for drug delivery and wound dressing applications. It is evident that formic acid is used as an organic volatile solvent to dissolve gelatin at room temperature for the electrospinning.

The use of gelatin nanofibers having enough tensile strength for fabricating nonwoven mats has received attention recently for use for antimicrobial applications [45–49]. Successful spinning of minimum diameter nanofibers results in the surface areas of these nanofibers being increased in addition to their light weight. This is basically required for wound dressings and other biomedical applications as listed in table 1. For instance Mindru *et al* [50] were successful in preparing nonwoven mats of required thickness and improved strengths for biomedical applications using a solvent system consisting of formic acid. Numerous questions have arisen however, due to use of cytotoxic solvents while preparing solutions for electrospinning of gelatin nanofibers to be used in real biomedical applications. Instead of cytotoxic solvents, Maleknia *et al* [51] used formic acid/water to prepare solutions for electrospinning of gelatin nanofibers for biomedical applications such as wound dressing, drug release, and tissue engineering. These authors were successful in spinning gelatin nanofibers with diameters as small as 197 nm. Chen *et al* [52] used formic acid and ethanol (to improve volatility of the solvent) instead of cytotoxic solvents while preparing the solvent for synthesizing electrospun gelatin nanofibers. These authors were successful in spinning gelatin nanofibers of 85 nm diameters, the lowest reported to date. During their investigations, they found that crosslinked gelatin nanofibers (after soaking the nanofibers in 2.5% of glutaraldehyde aqueous solution for 72 h and then being washed using de-ionized water before drying) were compatible with mouse mesangial cells. The drug delivery nanofibrous mats are required to be dissolved quickly in aqueous solutions. Aytac *et al* [42] found that the electrospun gelatin nanofibers encapsulated with ciprofloxacin/hydroxypropyl-beta-cyclodextrin-inclusion complex could dissolve faster in water than

Table 1. Use of ultrathin electrospun curcumin based nanofibers for biomedical applications.

About curcumin based nanofibers	Biomedical applications	References
Curcumin with polycaprolactone-polyethylene glycol nanofibers, Curcumin with poly(3-hydroxybutyric acid-co-3-hydroxyvaleric acid) (PHBV), Curcumin with poly(lactic acid)-hyperbranched polyglycerol, and Curcumin with ε-polycaprolactone/polyvinylalcohol multilayer nanofibers	Better wound healing potential	[17–20]
Curcumin with gum tragacanth/poly(ε-caprolactone) nanofibers	Improved antibacterial implementation and diabetic wound healing (*in vivo*)	[21]
Curcumin with almond gum/ polyvinyl alcohol (PVA) composite nanofibers	Improved bioavailability and therapeutic potential	[22]
Zinc-curcumin with coaxial nanofibers	As bone substitute	[23]
Curcumin with zein fibers	Improved antibacterial potential	[24]
Curcumin with cellulose acetate/polyvinylpyrrolidone nanofibers, Curcumin with polyurethanes nanofibers, and Curcumin with gelatin nanofibers	Antibacterial performance	[25–27]
Curcumin nanofibers	Anti-adhesion potential	[28]
Curcumin with chitosan/ poly (vinyl alcohol) (PVA) nanofibers	Drug delivery potential	[29]

electrospun gelatin nanofibers loaded with ciprofloxacin. Yabing *et al* [40] synthesized drugs (inhibitors such as SP600125, c-Jun N-terminal kinase and SB203580, p38 MAP kinase)-loaded micelles (poly(ethylene glycol)-block-caprolactone copolymer) using dialysis method and incorporated these drugs into electrospun gelatin nanofibers. The dual drugs delivery electrospun gelatin nanofibrous mats were used as scaffolds for the treatment of infections around the teeth. Nanofibrous mats prepared from electrospun nanofibers have large surface areas and they are expected to play a significant role in tissue engineering. The use of formic acid as a solvent for electrospinning biofunctional nanofibers has resulted in their use in various biomedical applications, such as immobilization of enzymes, bone regeneration materials, antibacterial and antifungal activities in release of drugs, encapsulation of bioactive materials during food packaging and wound dressing [53].

Turmeric is derived from *Curcuma longa* (common turmeric, an herbaceous plant) and has been widely used in India and China as a bioactive compound with powerful anti-inflammatory and antioxidant medicinal properties. Curcumin is one of the components of turmeric. It has been shown that synthetic dimethoxycurcumin is more potent to destroy cancer (a leading cause of every sixth death worldwide) cells than natural curcumin (derived from the plant) [54–64]. Ramírezagudelo *et al* [55] incorporated antibiotic doxycycline drugs (inhibitors of mitochondrial biogenesis, could restrict cancer stem cells in initial breast cancer stages) into electrospun hybrid poly-caprolactone/gelatin/hydroxyapatite soft nanofibrous mats and evaluated these drug delivery meshes as effective anti-tumor and antibacterial scaffolds. The use of formic acid as solvent for solutes such as curcumin and gelatin has been the preferred choice in many biomedical researches. Authors have prepared solutions of curcumin and dimethoxycurcumin using formic acid [54, 65–67]. Curcumin is a natural monomer (as shown in figure 1(a)), and nanofibers containing poly(curcumin) (as shown in figure 1(b)) can be used in medical treatments such as curing the skin injuries, as shown in figure 2(a). More curcumin would be expected to release with a specific rate from higher concentrations, such as 17% curcumin loaded poly (ε-caprolactone) (PCL) nanofibers than the lower concentrations, such as 3% curcumin loaded PCL nanofibers, after 12 h (as shown in figure 2(b)) [30]. Using PCL-curcumin solutions, biofunctional electrospun nanofibers were prepared [30–33, 68]. Hoang *et al* [68] fabricated curcumin loaded PCL/chitosan nonwoven mats (for wound dressings) using formic acid and acetone together as solvents while electrospinning nanofibers. They also investigated the release of curcumin (via an *in vitro* approach) from nonwoven mats of these fibers (having fiber diameters in the range between 267 nm to 402 nm); it was found to be nearly 80% during the initial 100 h. The gelatin nanofibers were found to serve as vehicles to release the drugs in controlled manner. These electrospun nanofibers were prepared in such a way that they had highly functionalized surface areas and their mats had excellent porosity to both, incorporate curcumin and allow curcumin diffusion out of the matrix, thereby improving their drug releasing capabilities. Xinyi *et al* [33] prepared curcumin/gelatin nanofibrous mats and investigated the release of curcumin on rat models (acute wounds) via *in vitro* approach, as shown in figure 2(c) [33]. While investigating crosslinked curcumin/gelatin nanofibers (after placing in a 25% glutaraldehyde solution with ethanol (1% v/v) before vacuum drying for 72 h at 4 °C), the authors found improved mechanical strength of this electrospun nanofibers, as shown in figure 3 [33].The wound healing was tested by treating rats using the curcumin/gelatin nanofibrous mats (healing analyses are shown in figure 4 for the 3rd, 7th, and 15th days after wounding). This encouraged us to prepare curcumin loaded gelatin nanofibers suitable for fabrication of nanofibrous mats for the application of sustained release of curcumin and oxygen to the wound (during healing).

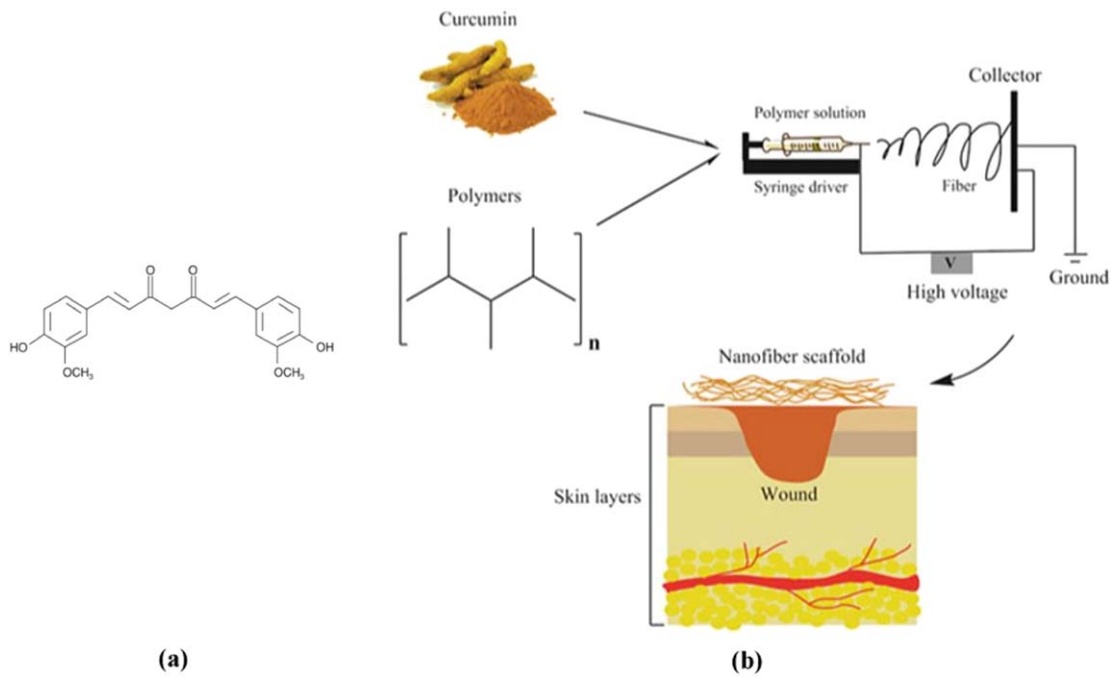

Figure 1. The biofunctional curcumin nanofibers. (a) Molecular structure of curcumin (1,7-bis(4-hydroxy-3-methoxyphenyl)-1,6-heptadiene-3,5-dione) (Reprinted with permission from [30]. Copyright 2009 John Wiley and Sons). (b) Application of curcumin-loaded nanofibers in wound healing (Reprinted with permission from [31]. Copyright 2018 John Wiley and Sons).

In the present study, an electrospining method was adapted to prepare the curcumin loaded gelatin nanofibers; characterizations of the nanofibers were done using scanning electron microscopy (SEM). Investigations were done to find the effects of critical process parameters such as distance between the spinneret and collector, polymer solution flow rate, voltage and viscosity on the preparation of uniform and ultrathin porous nanofibers having applications in wound dressings. In the present investigation the curcumin loaded gelatin nanofibers were selected in the hope of having improved mechanical and wound healing properties assuming these nanofibers should release the curcumin at appropriate rates which is of extreme importance to permit application of its biological effects during wound healing applications. It has been shown that the electrospun curcumin/gelatin nanofibers with lower diameters have larger surface area to volume ratios and porosity than larger diameter fibers and thus these nanofibers can be developed for sustained release of curcumin and oxygen (due to enough porosity) to the wound [31]. Curcumin/gelatin nanofibers can be further crosslinked for improved mechanical (tensile) strength (if required) for further development of nanofibrous mats for wound healing. These nanofibrous mats would have then anti-oxidant and anti-inflammatory features that could address wound healing in a very efficient way [31, 68–86].

1.2. Mechanism behind electrospinning of curcumin/gelatin nanofibers

Electrospinning uses an electric field which is applied across a spinneret and a ground electrode to withdraw a jet of polymer solution from the orifice of the spinneret. In electrospinning the Maxwell or electrical stress is given as $\frac{\varepsilon V^2}{d^2}$, where ε is the permittivity, V is the voltage, and d is the electrode separation. The critical voltage (V_c) which is $\sqrt{\frac{\gamma d^2}{\varepsilon R}}$, must be exceeded before any jet can spread out from the electrospinning tip. In particular, for $\gamma = 10^{-2} kg/s^2$, $d = 10^{-2}\, m$, $\varepsilon = 10^{-10} C^2/(Jm)$ and $R = 10^{-4} m$, a voltage of order 10 KV is required to form any jet [87].

Yeo *et al* [87] assumed *a priori* equilibrium conical shape for the Taylor cone (for the fluid drop) formation at the tip of the spinneret. The solution of the Laplace equation (used in the formulation) in the weak polarization limit describes the electrostatics in the fluid phases in an axisymmetric spherical coordinate system (r, θ, ϕ) with the vertex of the Taylor cone at the origin which can be shown using equation (1).

$$\varphi_l(r, \theta) = A_n\, r^n P_n(\cos\theta);\ \ for\ \theta_0 \geqslant \theta \geqslant 0,$$
$$\text{and}$$
$$\varphi_g(r, \theta) = B_n\, r^n P_n \cos(\pi - \theta);\ \ for\ \pi \geqslant \theta \geqslant \theta_0 \tag{1}$$

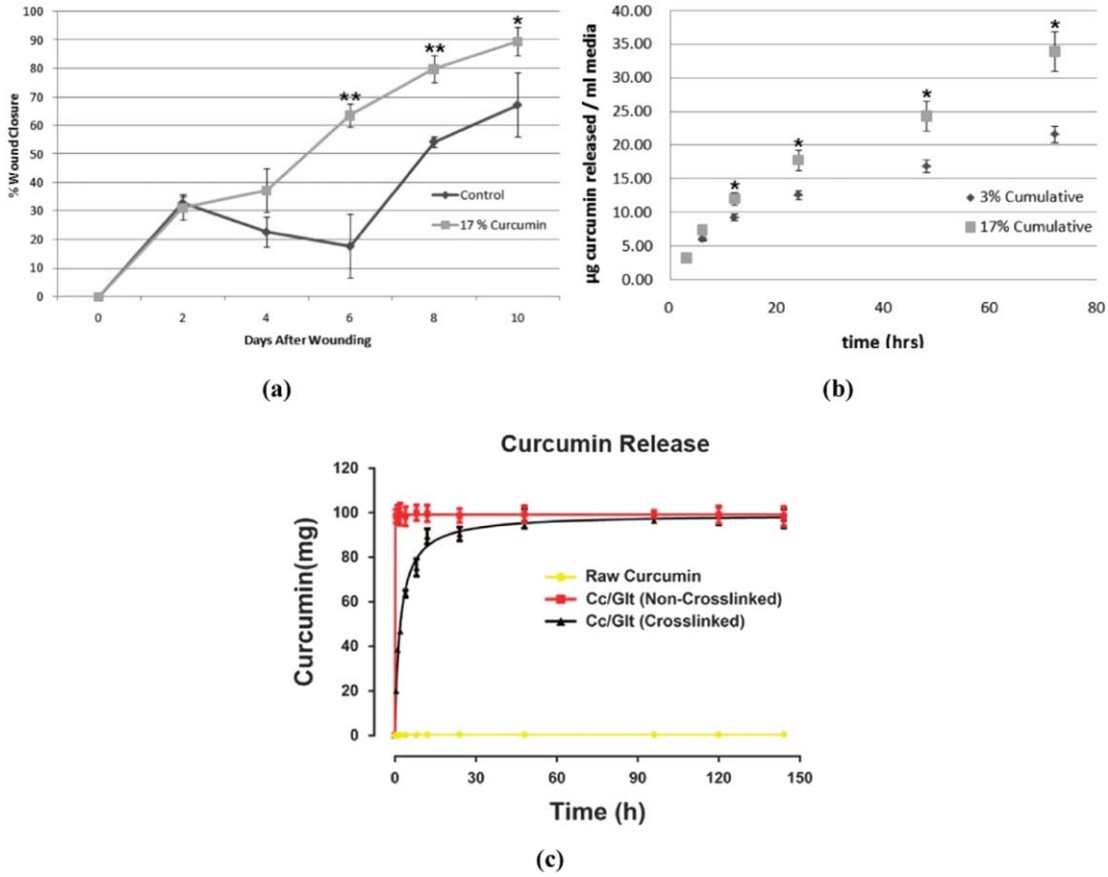

Figure 2. Release of curcumin with time. (a) Comparison of wound closure as a function of time. The wound was healed through release of curcumin from PCL nanofibers (Reprinted with permission from [30]. Copyright 2009 John Wiley and Sons). (b) *Plots of cumulative discharge of curcumin with time. Significant release of 17% curcumin from curcumin-loaded PCL nanofibers after 12 h (Reprinted with permission from [30]. Copyright 2009 John Wiley and Sons). (c) Release of curcumin from curcumin/gelatin nanofibrous mats as a function of time (*in vitro*) (Reprinted with permission from Ref. 33. Copyright 2017 Springer Nature). *Note: Pro 7.5 software program was used to analyze the release of curcumin from curcumin loaded Poly (ε-caprolactone) PCL nanofibers using one-way ANOVA with Tukey's test. $p \leqslant 0.05$ was considered significant.

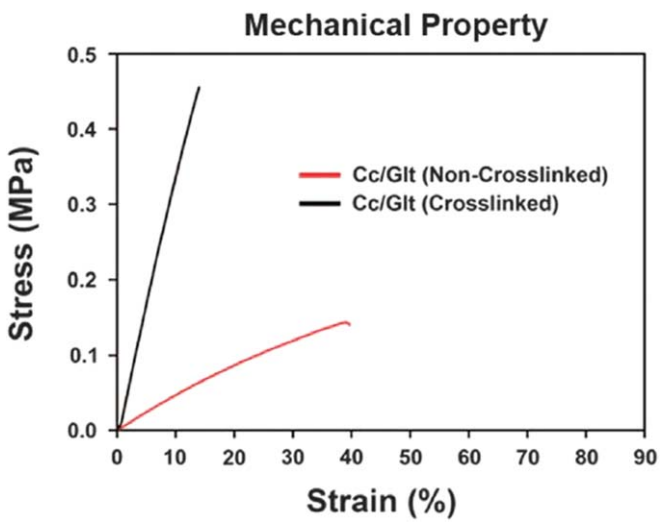

Figure 3. Crosslinked nanofibers having improved mechanical strength (Reprinted with permission from [33]. Copyright 2017 Springer Nature). CC BY 4.0

In the above equation (1), the volume of the fluid drop is given by $V = \frac{4}{3}\pi r^3$, where r is the distance from the cone vertex of angle $2\theta_0$ to the tip of the spinneret and the shape of drop is represented using a Taylor cone, thus r is characterized as $r = R(z)$. Further, the $z - axis$ is parallel to the applied electric field with $z \in [-l \quad l]$,

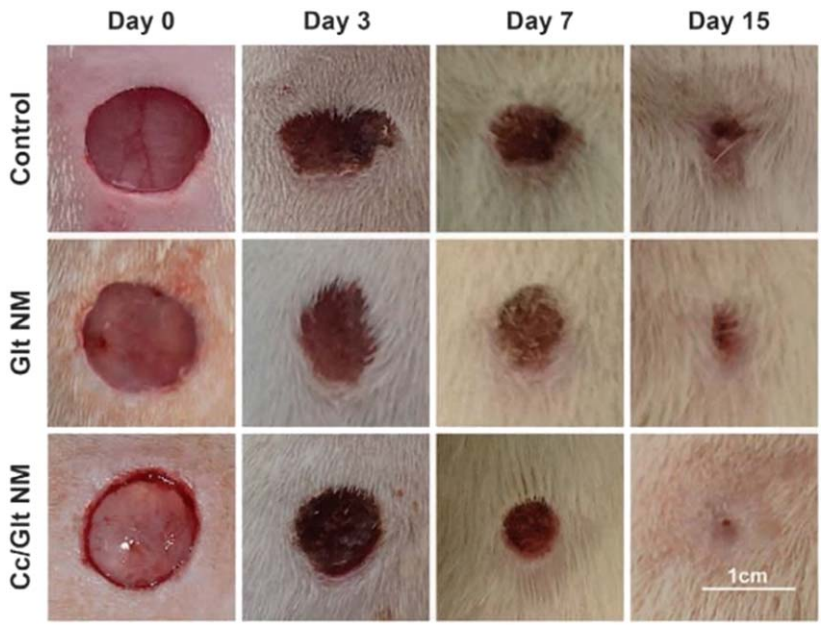

Figure 4. Wound (acute back-skin) closure (day-wise performance) after application of *curcumin/gelatin nanofibrous mats (NM) on rats (*in vivo*) (Reprinted with permission from [33]. Copyright 2017 Springer Nature. CC BY 4.0) *Note: Healing in three different ways: wound treated without mats (control) or using curcumin/gelatin (Cc/Glt) NM or using Glt NM. Wounds (6 mm in diameter) were created in the back (after they were shaved at their backs) of each rat.

where l is the length of the semi long axis of the drop and the boundary condition $\theta_0 \geqslant \theta \geqslant 0$ represents the region occupied by the fluid. $P_n[x]$ is the Legendre function, and A_n and B_n are constants. They suggested a model for electrospinning composite nanofibers which is based on a sink-like flow towards the vertex of the Taylor cone. The solution of the flow in axisymmetric polar coordinates $(r, \varepsilon, 0)$ was given using equations (2) and (3).

$$v_r = \frac{vF(\varepsilon)}{r} \tag{2}$$

$$F(\varepsilon) = b\left\{3\tanh^2\left[\left(\sqrt{\frac{-b}{2}}\right)(\alpha - \varepsilon) + 1.146\right] - 2\right\} \tag{3}$$

In the above equations (2) and (3), v_r is the radial velocity of flow, v is the kinematic viscosity of flow, α is the wedge/Taylor cone half angle, b is a parameter which determines the inertial concentration of flow into the Taylor cone vertex/Taylor cone. Mass and charge conservations led to expressions for v and σ in terms of R and E, and the momentum and E-field equations were recast using second-order differential equations. Slope of the jet surface (R') is supposed to be highest at the origin of the nozzle and thus initial value of z is equal to zero. Further, boundary conditions were set using the set of equation (4) [88, 89].

$$\begin{aligned} R(0) &= 1 \\ E(0) &= E_0 \\ \tau_{prr} &= 2r_\eta \frac{R_0'}{R_0^3} \\ \tau_{pzz} &= -2\tau_{prr} \end{aligned} \tag{4}$$

In the above equation (4), R_0 is the initial radius of jet and the jet velocity (υ_0) is calculated using the formula $\upsilon_0 = \frac{Q}{\pi R_0^2 K}$, where Q is the flow rate of the solution, and K is the conductivity of liquid solution. The electric field (E_0) is calculated using the formula $E_0 = \frac{I}{\pi R_0^2 K}$ and the surface charge density (σ_0) is calculated using the formula $\bar{\varepsilon}E_0$, where $\bar{\varepsilon}$ is the dielectric constant of ambient air and E_0 is the constant to be used during simulation of the electrospinning. The viscous stress (τ_0) is calculated using the formula $\tau_0 = \frac{\eta_0 \upsilon_0}{R_0}$. A power-law fluid is a generalized Newtonian fluid and for that the shear stress (τ), is given as $\tau = K'\left(\frac{\partial v}{\partial y}\right)^m$. It is observed that the electric field is induced by the surface charge gradient and thus it is insensitive to the thinning of the electrospun jet, as shown in equation (5) [88].

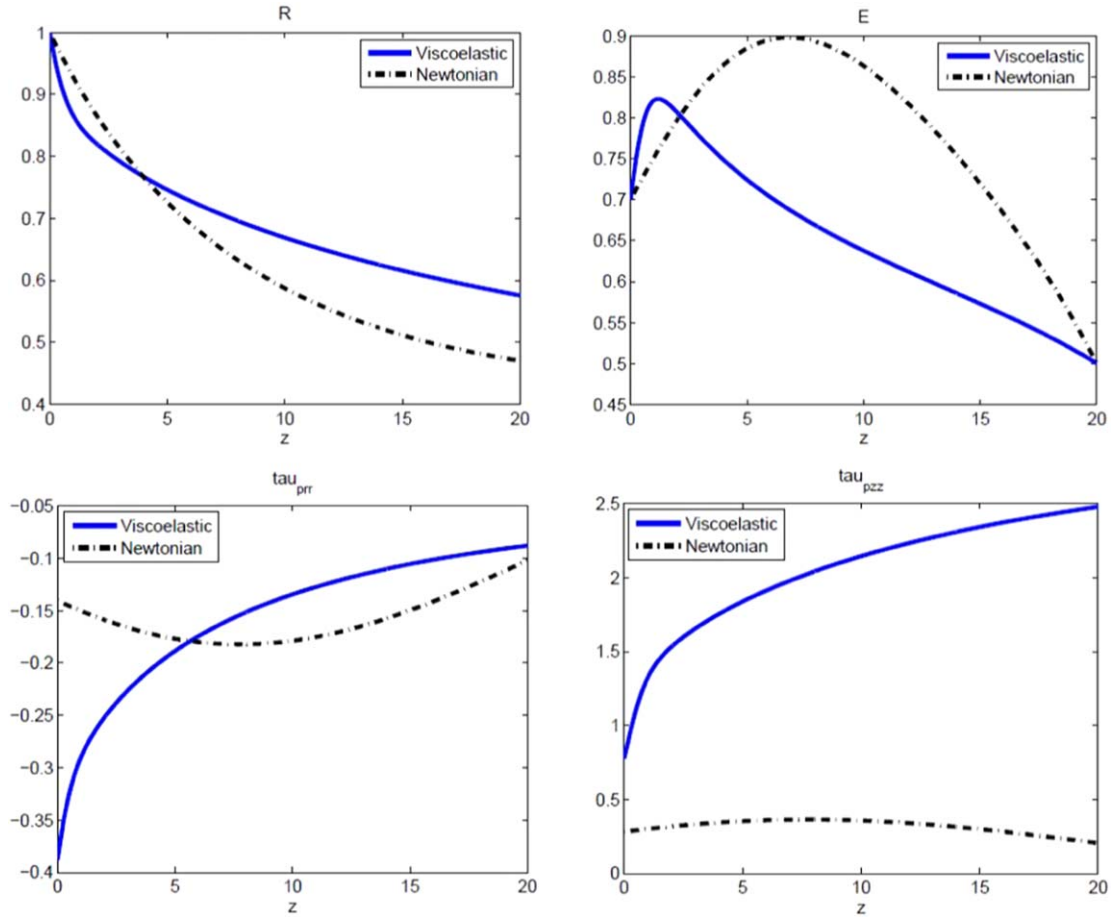

Figure 5. Plots showing behavior of process parameters as functions of axial position (Reprinted with permission from [88]. Copyright 2014 Romanian Academy Publishing House).

$$\frac{d(\sigma R)}{dz} \simeq -\left(2R\frac{dR}{dz}\right)/Pe \tag{5}$$

Thus, the variation of E with respect to axial position (z) can be shown using equation (6) [88].

$$\frac{d(E)}{dz} = \ln \chi\left(\frac{d^2R^2}{dz^2}\right)/Pe \tag{6}$$

In figure 5 plots are shown for the changes of various parameters, radius of jet (R), electric field (E), radial normal stress (τ_{prr}) and axial viscous normal stress (τ_{pzz}) with the respect to axial position (Z). It is observed that the electric field (E) increased to a peak and then relaxed to some extent. The model discussed so far was shown to be capable of predicting the behavior of the process parameters of electrospinning [88]. Through these plots the flow procedure in relation to the jetting process involved in the electric field is outlined.

1.3. Applications of biofunctional curcumin nanofibers

Ultrathin porous nanofibrous mats can be prepared using electrospinning for various biomedical applications. Various researchers have emphasized the curcumin based nanofibers in their investigations to find their potential uses in wound healing, drug-delivery and antibacterial applications (as shown in table 1). The structures of these electrospun nanofibers can be tailored for large surface area and length up to kilometers using the electrostatically driven jet of polymer solution. Further, it was found that bioactive molecules of graphene oxide and a Zn-curcumin complex, when combined with the electrospun nanofibers, had potential application in bone regeneration, as shown in table 1.

2. Electrospinning of curcumin/gelatin nanofibers

The electrospinning set-up we used is shown in figure 6(a). There were four components associated with the electrospinning process: spinneret, voltage supply, drum collector and dispenser. In our electrospinning process

a voltage gradient is set across the length of the drum collector (loaded with an aluminium sheet), and a polymeric solution (taken in a 2 ml syringe) is placed in the dispensor. Nanofibers are stretched out from the polymeric solution containing a polar organic solvent and a polymer solute in the desired amounts. These nanofibers are collected over the drum collector which is rotated at a speed around 1000 rpm to reduce the nanofibers diameter by stretching them and aligning them linearly in addition to improving their mechanical properties. During this process, four critical parameters, distance, flow rate, voltage and viscosity, are taken into consideration. These were our control parameters in preparation of the biofunctional nanofibers.

A polymeric solution was prepared by mixing 1% curcumin (0.1 g) with 1.5% gelatin (0.15 g) in 10 ml of formic acid, HCOOH (98% concentrated). Another polymeric solution was prepared by mixing 1.2% curcumin (0.12 g) with 2% gelatin (0.2 g) in 10 ml of formic acid, HCOOH (98% concentrated), both at room temperature. The experiments were conducted at room temperature, in ambient air which had moisture around 80%. Nanofibers were prepared by varying the distance between the spinneret (10 cm and 15 cm), flow rate (0.1 ml h^{-1} and 0.15 ml h^{-1}), voltage (15 KV and 20 KV), and viscosity (65 cP and 70 cP, due to the additives concentrations). The mats were dried at room temperature for 48 h to completely remove the formic acid before characterization. The diameters of the nanofibers were then measured using scanning electron microscopy (SEM) (the set-up is shown in figure 6(b)).

3. Results and discussions

The diameters (nm) of the nanofibers prepared during the electrospinning processes are shown in table 2. The significant trends in the results (in terms of the diameters of the nanofibers) observed were as follows: at a higher voltage, such as 15 KV (at 15 cm distance, 0.1 ml h^{-1} flow rate and 65 cP viscosity) using a solution having 1.5% gelatin, 1% curcumin in 10 ml of 98% concentrated formic acid, the diameters of the nanofibers were around 254 nm (254 $\pm$ 28 nm) which is considerably higher than the 181 nm (181 $\pm$ 66 nm) (as shown in figure 6(c)) diameter obtained at 10 KV using the same solution and keeping the other parameters the same. At a higher flow rate, such as 0.15 ml h^{-1} (at 10 cm distance, 15 KV voltage and 65 cP viscosity) using a solution having 1.5% gelatin, 1% curcumin in 10 ml of 98% concentrated formic acid, the diameters of nanofibers were measured around 147 nm (147 $\pm$ 34 nm) (as shown in figure 6(d)) which is considerably lower than 260 nm (260 $\pm$ 26.5 nm) as the diameter obtained at 0.1 ml h^{-1} flow rate using the same solution and keeping the other parameters the same. At a higher flow rate, such as 0.15 ml h^{-1} (at 15 cm distance, 10 KV voltage and 70 cP viscosity) using a solution having 2% gelatin, 1.2% curcumin in 10 ml of 98% concentrated formic acid, the diameters of nanofibers were measured around 206 nm (206 $\pm$ 56 nm) (as shown in figure 6(e)) which is only slightly lower than 229.5 nm (229.5 $\pm$ 60 nm) (as shown in figure 6(f)) as the diameter obtained at 0.1 ml h^{-1} (at 15 cm distance, 15 KV voltage and 70 cP viscosity) using the same solution. For a higher concentration (2% gelatin, 1.2% curcumin in 10 ml of 98% concentrated formic acid), the viscosity was measured (using a viscosity meter) to be 70 cP and then the diameter of the fibers increased to 235 nm (235 $\pm$ 47 nm) (as shown in figure 6(g)), at 10 cm distance, 0.15 ml h^{-1} flow rate and 15 KV voltage, from 147 nm (147 $\pm$ 34 nm) (as shown in figure 6(d)) (measured at 1.5% gelatin, 1% curcumin in 10 ml *of* 98% concentrated formic acid) at 10 cm distance, 0.15 ml h^{-1} flow rate, 15 KV voltage and 65 cP viscosity. At a higher distance, such as 15 cm (0.15 ml h^{-1} flow rate, 15 KV voltage *and* 70 cP viscosity) using a solution having 2% gelatin, 1.2% curcumin in 10 ml *of* 98% concentrated formic acid, the diameters of nanofibers were measured around 274 nm (274 $\pm$ 53 nm) (as shown in figure 6(h)) which is higher than the 235 nm (235 $\pm$ 47 nm) (as shown in figure 6(g)) diameter obtained for 10 cm distance using the same solution and keeping the other parameters the same.

3.1. Design of experiments

The 2^k factorial design was implemented to conduct the experiments after considering the four independent variables (each varied at two different levels i.e. low (−) and high (+)); these were the distance between the spinneret and collector, flow rate, voltage and viscosity [90–92]. Thus, the total number of observations were 2^4 i.e. 16.

All 16 samples were examined under scanning electron microscopy (SEM) for diameters in nanometers (as shown in table 2). A few sample images of the curcumin/gelatin nanofibers examined under SEM are shown in figures 6(c)–(h). The ultrathin porous nanofibers membranes were prepared under all process conditions.

3.2. Analysis of variance

It was done to find the significance of the contributions of the individual parameters in achieving the minimum diameter of the nanofibers. Calculations for the correction factor, CF (to compute the sum of squares of input variables) were conducted using equation (7).

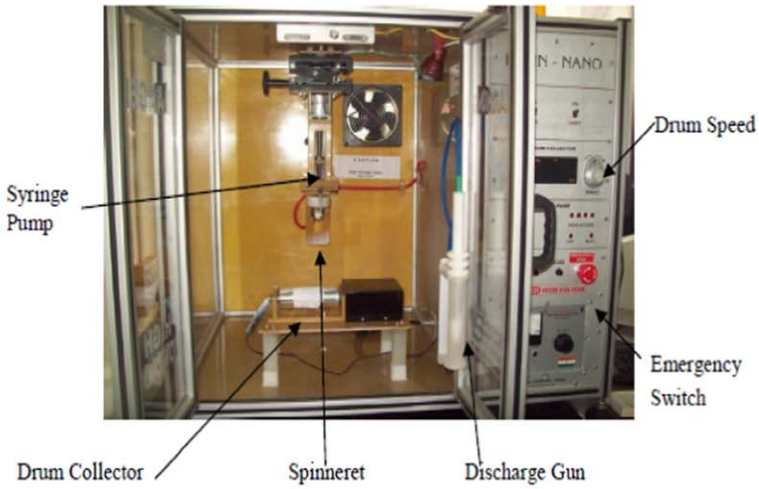

Specifications	*Model –VI*
Power Supply Voltage (*KV*)	*0-40 KV* *1Ma*
Syringe Size Needle	*2,5,10,* and *20 mL* Disposal Syringes
Flow Rate (*mL/h*)	From *0.05* up to *100 mL/h* dependent *upon syringe type*
Collector Drum $(l \times dia.)$ **(*mm*)**	125×40
Disc diameter Plate $(l \times b)$ **(*mm*)**	100×100

(a)

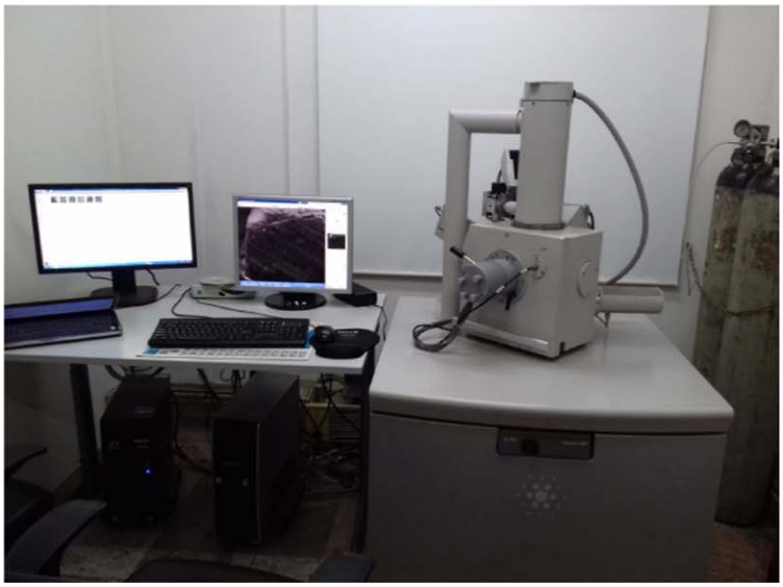

SEM Series	**FEI QUANTA 200 with EDS**
Product Version	*4.1.13.2167*
Mode of Operation	High vacuum, Low vacuum and ESEM
Magnification	*2,00000 X*

(b)

Figure 6. The electrospun curcumin/gelatin nanofibers. (a) *Electrospinning set-up and its specifications. (b) SEM set-up and its specifications. (c) Sample 2: 15 cm, 0.1 ml h^{-1}, 10 KV and 65 cP: 181 nm (181 ± 66 nm) average fiber diameter. (d) Sample 7: 10 cm, 0.15 ml h^{-1}, 15 KV and 65 cP: 147 nm (147 ± 34 nm) average fiber diameter. (e) Sample 12: 15 cm, 0.15 ml h^{-1}, 10 KV and 70 cP: 206 nm (206 ± 56 nm) average fiber diameter. (f) Sample 14: 15 cm, 0.1 ml h^{-1}, 15 KV and 70 cP: 229.5 nm (229.5 ± 60 nm) average fiber diameter. (g) Sample 15: 10 cm, 0.15 ml h^{-1}, 15 KV and 70 cP: 235 nm (235 ± 47 nm) average fiber diameter. (h) Sample 16: 15 cm, 0.15 ml h^{-1}, 15 KV and 70 cP: 274 nm (274 ± 53 nm) average fiber diameter. *Note: The electrospinning chamber is provided with a residual charge discharge gun/stick which is used to remove/short static charges for safe operations.

3.2.1. Correction factor (CF)

The CF for diameter (nm) was calculated as

$$CF = \frac{(\sum X)^2}{n} = \frac{(4085.5)^2}{16} \cong 1043207 \tag{7}$$

Where, the $\sum X$ is the gross total of observed diameters and n is the number of iterations, i.e. 16 (both as shown in table 2)

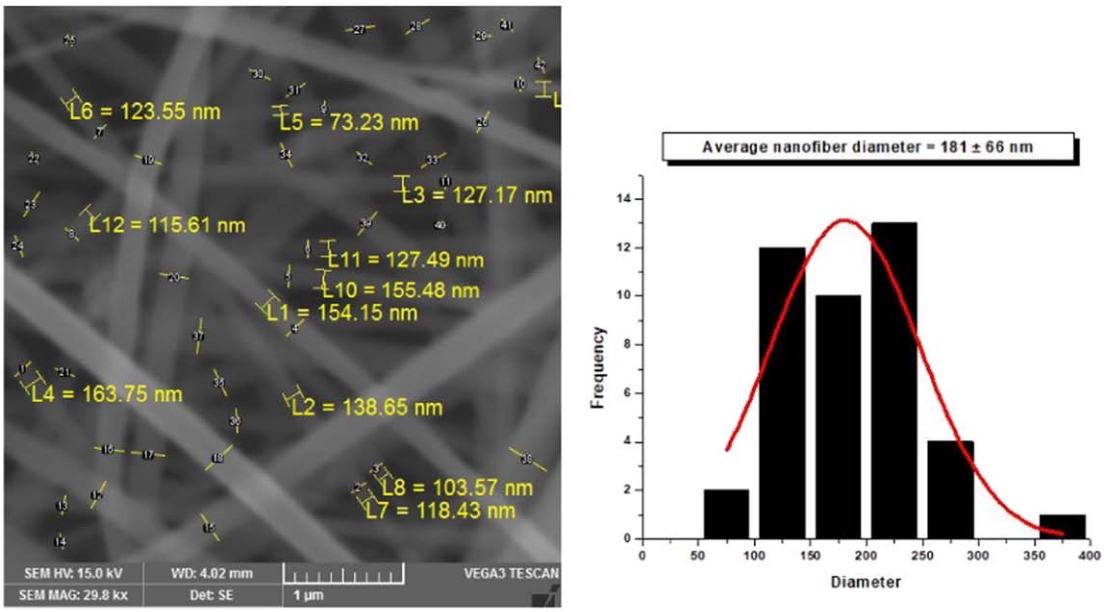

(c)

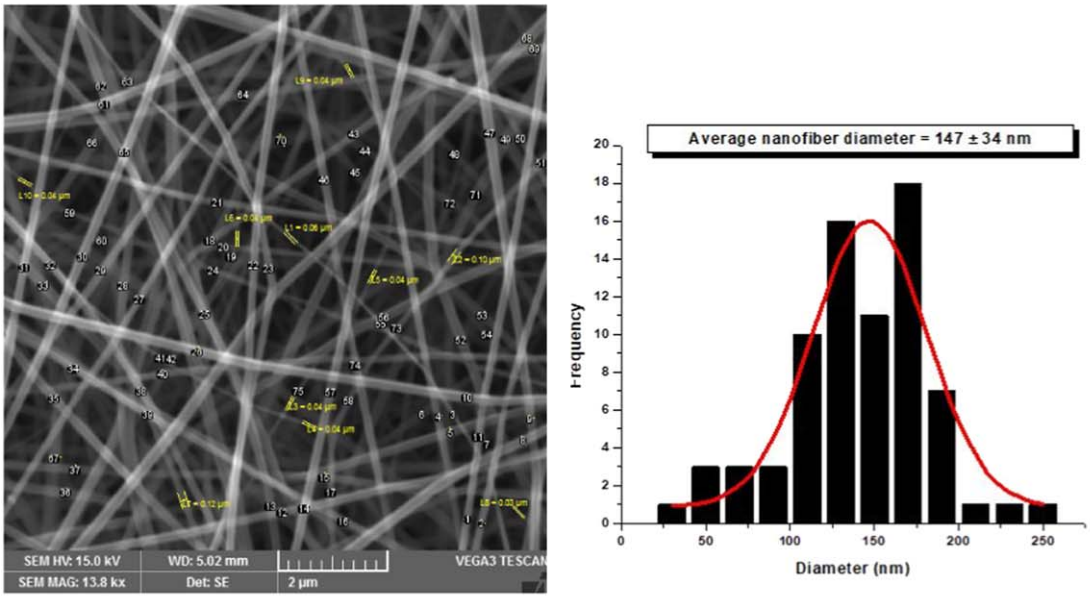

(d)

Figure 6. (Continued.)

The effect of the factors can be given using equation (8).

$$\frac{[\sum Y_{low}]^2}{n} + \frac{\left[\sum Y_{high}\right]^2}{n} - CF \tag{8}$$

Where, Y is an input variable, such as the distance (A), and Y_{high} and Y_{low} stand for the sum of all average diameters prepared at high (+) and low (−) levels, respectively, for the particular input variable with each sum taken over the high and low values of the other variables. The corresponding values of average diameters for the high (+) and low (−) levels of the particular input variable were taken from table 2.

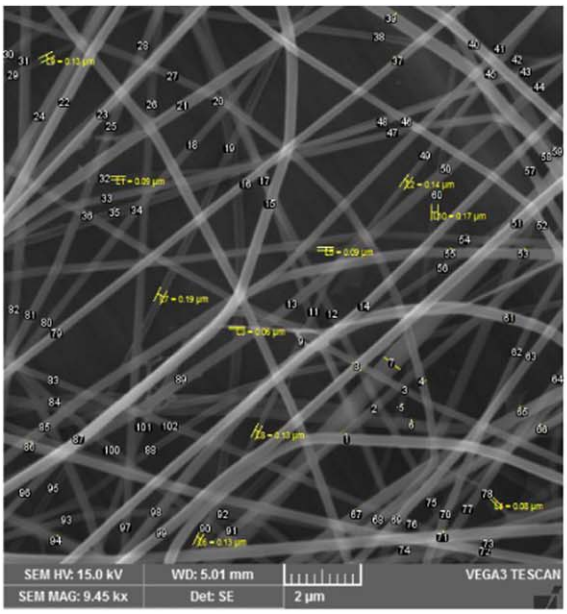

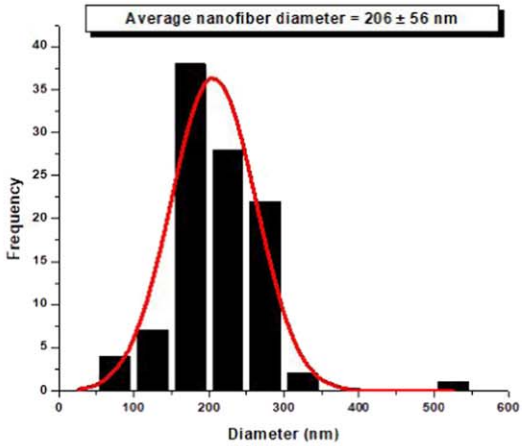

(e)

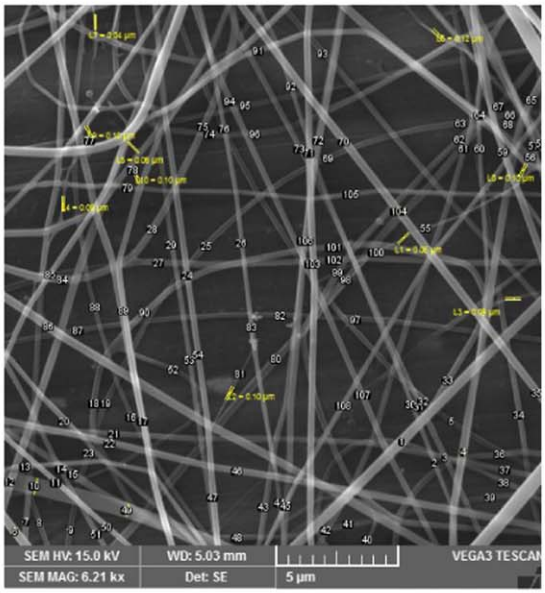

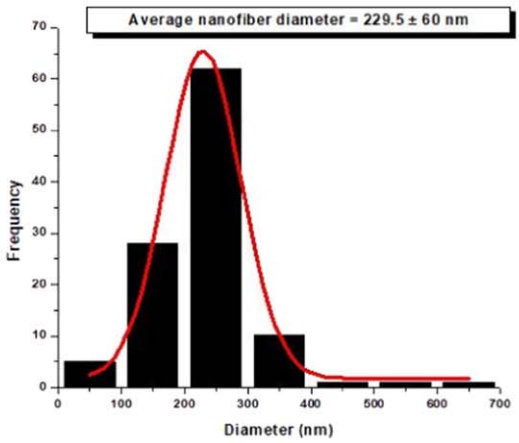

(f)

Figure 6. (Continued.)

1. Sum of squares, distance factor (cm), SS_A

$$\frac{[\sum A_{low}]^2}{n} + \frac{[\sum A_{high}]^2}{n} - CF$$
$$= \frac{[205 + 270 + 260 + 147 + 287 + 375 + 308 + 235]^2}{8}$$
$$+ \frac{[181 + 280 + 254 + 286 + 288 + 206 + 229.5 + 274]^2}{8}$$
$$- 1043207 = 489.5$$

Similarly,

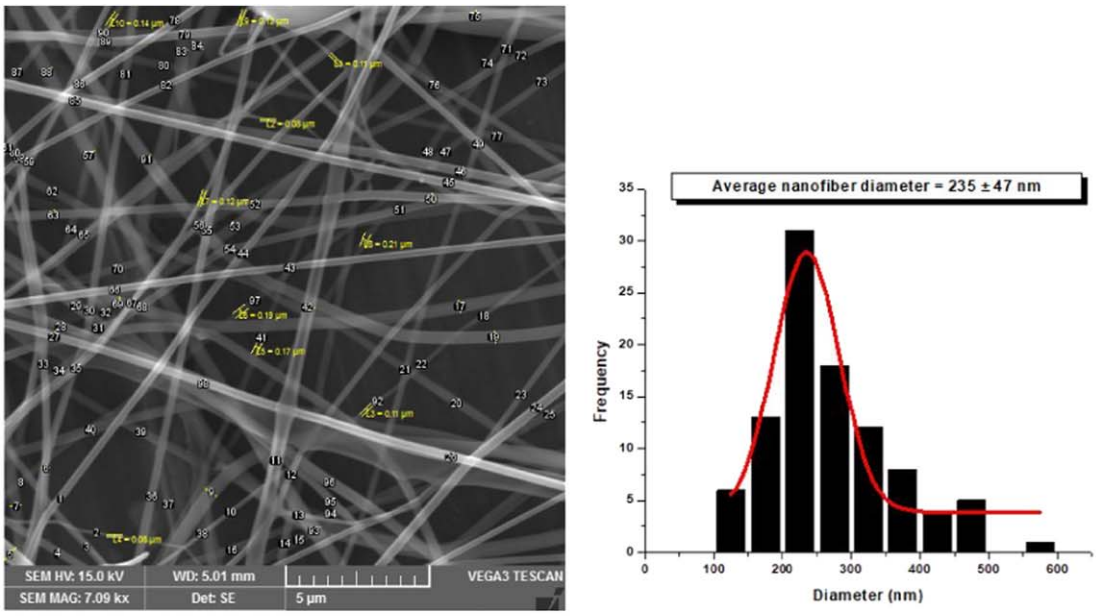

(g)

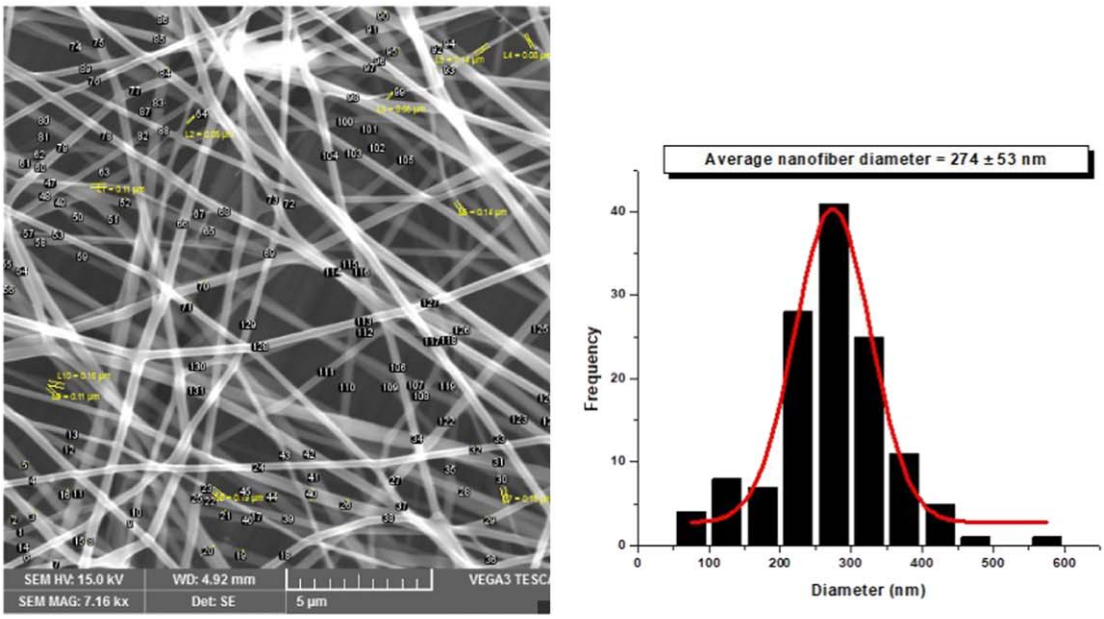

(h)

Figure 6. (Continued.)

2. Sum of squares, flow rate factor (ml h^{-1}), SS_B

$$\frac{[\sum B_{low}]^2}{n} + \frac{\left[\sum B_{high}\right]^2}{n} - CF = 228.5$$

3. Sum of squares, voltage factor (KV), SS_C

$$\frac{[\sum C_{low}]^2}{n} + \frac{\left[\sum C_{high}\right]^2}{n} - CF = 606$$

Table 2. Results of experiments.

Iteration No.	Distance (cm) A	Flow Rate (mL/h) B	Voltage (KV) C	[a]Viscosity (cP) D	Average Diameters (nm)
1	(−)10	(−)0.1	(−)10	(−)65	205 ± 22.5
2	(+)15	(−)0.1	(−)10	(−)65	181 ± 66
3	(−)10	(+)0.15	(−)10	(−)65	270 ± 16
4	(+)15	(+)0.15	(−)10	(−)65	280 ± 20
5	(−)10	(−)0.1	(+)15	(−)65	260 ± 26.5
6	(+)15	(−)0.1	(+)15	(−)65	254 ± 28
7	(−)10	(+)0.15	(+)15	(−)65	147 ± 34
8	(+)15	(+)0.15	(+)15	(−)65	286 ± 31
9	(−)10	(−)0.1	(−)10	(+)70	287 ± 77
10	(+)15	(−)0.1	(−)10	(+)70	288 ± 57
11	(−)10	(+)0.15	(−)10	(+)70	375 ± 96
12	(+)15	(+)0.15	(−)10	(+)70	206 ± 56
13	(−)10	(−)0.1	(+)15	(+)70	308 ± 74
14	(+)15	(−)0.1	(+)15	(+)70	229.5 ± 60
15	(−)10	(+)0.15	(+)15	(+)70	235 ± 47
16	(+)15	(+)0.15	(+)15	(+)70	274 ± 53
					$Total \sum X = 4085.5$

[a] Where, (+) indicates high value and (−) indicates low value of parameters.
*Note: Change in concentration of curcumin (from 1% to 1.2%) and gelatin (from 1.5% to 2%) increased the viscosity (from 65 cP to 70 cP). The effect of concentration is mapped in terms of viscosity.

4. Sum of squares, viscosity factor (cP), SS_D

$$\frac{[\sum D_{low}]^2}{n} + \frac{\left[\sum D_{high}\right]^2}{n} - CF = 6380$$

To examine the interaction, table 3 was formulated. The Sum of squares for each pair of interactions is given using equation (9).

$$\frac{[\sum AB_{low}]^2}{n} + \frac{\left[\sum AB_{high}\right]^2}{n} - CF \tag{9}$$

Where, AB represents interaction between distance (cm), A, and flow rate (ml h^{-1}), B. The corresponding values of average diameters for the high (+) and low (−) levels of the particular interaction between variables were taken from table 3.

The values of the sum of squares for the various interactions are as follows

1. Sum of squares for interaction AB, SS_{AB}

$$\begin{aligned}&\frac{[\sum AB_{low}]^2}{n} + \frac{\left[\sum AB_{high}\right]^2}{n} - CF\\ &= \frac{[181 + 270 + 254 + 147 + 288 + 375 + 229.5 + 235]^2}{8}\\ &+ \frac{[205 + 280 + 260 + 286 + 287 + 206 + 308 + 274]^2}{8}\\ &- 1043207 = 1000\end{aligned}$$

Similarly,

2. Sum of squares for interaction AC, SS_{AC}

$$\frac{[\sum AC_{low}]^2}{n} + \frac{\left[\sum AC_{high}\right]^2}{n} - CF = 4743.5$$

Table 3. Interaction table (curcumin nanofibers).

S. no.	*AB*	*AC*	*AD*	*BC*	*BD*	*CD*	*ABC*	*BCD*	*ACD*	*ABCD*	Diameters (nm) as in table 2
1	+	+	+	+	+	+	—	—	—	+	**205 ± 22.5**
2	—	—	—	+	+	+	+	—	+	—	**181 ± 66**
3	—	+	+	—	—	+	+	+	—	—	**270 ± 16**
4	+	—	—	—	—	+	—	+	+	+	**280 ± 20**
5	+	—	+	—	+	—	+	+	+	—	**260 ± 26.5**
6	—	+	—	—	+	—	—	+	—	+	**254 ± 28**
7	—	—	+	+	—	—	—	—	+	+	**147 ± 34**
8	+	+	—	+	—	—	+	—	—	—	**286 ± 31**
9	+	+	—	+	—	—	—	+	+	—	**287 ± 77**
10	—	—	+	+	—	—	+	+	—	+	**288 ± 57**
11	—	+	—	—	+	—	+	—	+	+	**375 ± 96**
12	+	—	+	—	+	—	—	—	—	—	**206 ± 56**
13	+	—	—	—	—	+	+	—	—	+	**308 ± 74**
14	—	+	+	—	—	+	—	—	+	—	**229.5 ± 60**
15	—	—	—	+	+	+	—	+	—	—	**235 ± 47**
16	+	+	+	+	+	+	+	+	+	+	**274 ± 53**

1. Sum of squares for interaction *AD*, SS_{AD}

$$\frac{[\sum AD_{low}]^2}{n} + \frac{\left[\sum AD_{high}\right]^2}{n} - CF = 6662.5$$

2. Sum of squares for interaction *BC*, SS_{BC}

$$\frac{[\sum BC_{low}]^2}{n} + \frac{\left[\sum BC_{high}\right]^2}{n} - CF = 4882.5$$

3. Sum of squares for interaction *BD*, SS_{BD}

$$\frac{[\sum BD_{low}]^2}{n} + \frac{\left[\sum BD_{high}\right]^2}{n} - CF = 695.5$$

4. Sum of squares for interaction *CD*, SS_{CD}

$$\frac{[\sum CD_{low}]^2}{n} + \frac{\left[\sum CD_{high}\right]^2}{n} - CF = 907.5$$

5. Sum of squares for interaction *ABC*, SS_{ABC}

$$\frac{[\sum ABC_{low}]^2}{n} + \frac{\left[\sum ABC_{high}\right]^2}{n} - CF = 9925$$

6. Sum of squares for interaction *BCD*, SS_{BCD}

$$\frac{[\sum BCD_{low}]^2}{n} + \frac{\left[\sum BCD_{high}\right]^2}{n} - CF = 2769$$

7. Sum of squares for interaction *ACD*, SS_{ACD}

$$\frac{[\sum ACD_{low}]^2}{n} + \frac{\left[\sum ACD_{high}\right]^2}{n} - CF = 21$$

Table 4. Effect estimation-final ANOVA table.

Remark	MODEL/ ERROR	Factor/ Interaction	Effect estimation	Sum of square (SOS)	% Contribution
Factors/interactions having significant contributions	**MODEL**	***ABC***	50	9925	**24**
	MODEL	***AD***	−41	6662.5	**16**
	MODEL	***D***	40	6380	**15.5**
	MODEL	***BC***	−35	4882.5	**12**
	MODEL	***AC***	34.5	4743.5	**11.5**
	MODEL	***BCD***	26	2769	**6.7**
	MODEL	***ABCD***	22	1947	**4.7**
	MODEL	***AB***	16	1000	**2.4**
	MODEL	***CD***	−15	907.5	**2.2**
	MODEL	***BD***	−13	695.5	**1.7**
	MODEL	***C***	−12	606	**1.5**
	MODEL	***A***	−11	489.5	**1.2**
	MODEL	***B***	7.5	228.5	**0.5**
Factor/interaction NOT having significant contribution	**ERROR**	***ACD***	−2	21	**0.05**
				$\sum SOS = 41257.5$	

8. Sum of squares for interaction *ABCD*, SS_{ABCD}

$$\frac{[\sum ABCD_{low}]^2}{n} + \frac{\left[\sum ABCD_{high}\right]^2}{n} - CF = 1947$$

Highest value = 9925 for ABC interaction

Errors, which are listed in table 4 can be pooled together and the *Ratio*, MS_{error} can be calculated using the equation (10).

$$MS_{error} = SS_{error} / V_{error} = 21 \tag{10}$$

Where, V_{error} represents the number of errors, and in our case it is one.

Now, in the calculation of the *F ratio*, using the *F-distribution* table, we have found the *F value* for 95% level of confidence as 7.71 and further concluded that the diameter primarily depends upon factors: (a) *ABC*-Interaction between distance (cm), flow rate (ml h^{-1}) and voltage (KV), (b) *AD*-Interaction between distance (cm) and viscosity (cP), (c) *D*-Viscosity (cP), (d) *BC*-Interaction between flow rate (ml h^{-1}) and voltage (KV), (e) *AC*-Interaction between distance (cm) and voltage (KV), (f) *BCD*-Interaction between flow rate (ml h^{-1}), voltage (KV) and viscosity (cP), (g) *ABCD*-Interaction between distance (cm), flow rate (ml h^{-1}), voltage (KV) and viscosity (cP), (h) *AB*-Interaction between distance (cm) and flow rate (ml h^{-1}), (i) *CD*-Interaction between voltage (KV) and viscosity (cP), (j) *BD*-Interaction between flow rate (ml h^{-1}) and viscosity (cP), (k) *C*-Voltage (KV), (l) *A*-Distance (cm), and (m) *B*-Flow rate (ml h^{-1}). These are treated as models and further tested for their contribution to the diameters of nanofibers (nm) (at 5% level of significance) in table 4. During the effect estimation, it is found about the factor *ACD*-Interaction between distance (cm), voltage (KV) and viscosity (cP) that it affects the diameter (nm) by 0.05% which is not significant and thus it is indicated as an error in table 4.

3.3. Regression analysis

As each input variable has two levels i.e. high (+) and low (−) levels and has one degree of freedom, thus an ordinary regression model was employed to calculate the minimum diameter of nanofibers after substitution of suitable values of the interaction effects such as β_1, β_2, β_4, β_5, β_6, β_7, β_8, β_9, and β_{10} (in terms of contributions of interactions between *ABC*-Interaction between distance (cm), flow rate (ml h^{-1}) and voltage (KV), *AD*-Interaction between distance (cm) and viscosity (cP), *BC*-Interaction between flow rate (ml h^{-1}) and voltage (KV), *AC*-Interaction between distance (cm) and voltage (KV), *BCD*-Interaction between flow rate (ml h^{-1}), voltage (KV) and viscosity (cP), *ABCD*-Interaction between distance (cm), flow rate (ml h^{-1}), voltage (KV) and viscosity (cP), *AB*-Interaction between distance (cm) and flow rate (ml h^{-1}), *CD*-Interaction between voltage (KV) and viscosity (cP), *BD*-Interaction between flow rate (ml h^{-1}) and viscosity (cP), respectively) as well as the main effects, such as β_3, β_{11}, β_{12}, and β_{13} (in terms of contributions of *D*-Viscosity (cP), *C*-Voltage (KV), *A*-Distance (cm), and *B*-Flow rate (ml h^{-1}), respectively), in equation (11).

$$Y = \beta_0 + \beta_1 X_1 + \beta_2 X_2 + \beta_3 X_3 + \ldots + \beta_n X_n + \xi \tag{11}$$

Where,

$$\beta_0 = \sum_{i=1}^{N} \frac{Y_i}{N} = \frac{4085.5}{16} = 255.344$$

Further, the effect of each factor, P, was calculated using the formula $Y_P = \bar{Y}_{P+} - \bar{Y}_{P-}$, where, $\bar{Y}_{P+}$ and $\bar{Y}_{P-}$ stand for the sums of all average diameters prepared at high (+) and low (−) levels, respectively, for the particular input variable. The corresponding values of the average diameters for the high (+) and low (−) levels of the particular input variable were taken from tables 2 and 3.

As an example, the effect of factor B can be calculated as follows:

$$\begin{aligned} D &= \bar{Y}_{D+} - \bar{Y}_{D-} \\ &= \frac{[287 + 288 + 375 + 206 + 308 + 229.5 + 235 + 274]}{8} \\ &- \frac{[205 + 181 + 270 + 280 + 260 + 254 + 147 + 286]}{8} = 40 \end{aligned}$$

Similarly, the effects of the other factors, such as ABC, AD, BC, AC, BCD, $ABCD$, AB, CD, BD, C, A, B, and ACD were calculated as 50, −41, −35, 34.5, 26, 22, 16, −15, −13, −12, −11, 7.5, and −2, respectively (as shown in table 4).

Therefore, the % *contribution for ABC* = (9925/41257.5) × 100 = 24

$$\beta_1 = \frac{1}{2}(\textit{effect estimate for factor } ABC) = 25$$

$$\beta_2 = \frac{1}{2}(\textit{effect estimate for factor } AD) = -20.5$$

$$\beta_3 = \frac{1}{2}(\textit{effect estimate for factor } D) = 20$$

$$\beta_4 = \frac{1}{2}(\textit{effect estimate for factor } BC) = -17.75$$

$$\beta_5 = \frac{1}{2}(\textit{effect estimate for factor } AC) = 17.25$$

$$\beta_6 = \frac{1}{2}(\textit{effect estimate for factor } BCD) = 13$$

$$\beta_7 = \frac{1}{2}(\textit{effect estimate for factor } ABCD) = 11$$

$$\beta_8 = \frac{1}{2}(\textit{effect estimate for factor } AB) = 8$$

$$\beta_9 = \frac{1}{2}(\textit{effect estimate for factor } CD) = -7.5$$

$$\beta_{10} = \frac{1}{2}(\textit{effect estimate for factor } BD) = -6.5$$

$$\beta_{11} = \frac{1}{2}(\textit{effect estimate for factor } C) = -6$$

$$\beta_{12} = \frac{1}{2}(\textit{effect estimate for factor } A) = -5.5$$

$$\beta_{13} = \frac{1}{2}(\textit{effect estimate for factor } B) = 3.75$$

The general form of the regression analysis equation is shown in equation (12). The minimum diameter of curcumin/gelatin nanofibers (nm) attainable using our system, can be calculated after substituting the suitable values of the coefficients (such as β_1, β_2, β_4, β_5, β_6, β_7, β_8, β_9, and β_{10}) of the interaction effects (such as X_{ABC}, X_{AD}, X_{BC}, X_{AC}, X_{BCD}, X_{ABCD}, X_{AB}, X_{CD}, and X_{BD}) as well as the coefficients (such as β_3, β_{11}, β_{12}, and β_{13}) of the main effects (such as X_D, X_C, X_A, and X_B) in equation (12).

$$\begin{aligned} \textit{Diameter } (nm) = {} & 255.344 + 25X_{ABC} - 20.5X_{AD} + 20X_D - 17.75X_{BC} \\ & + 17.25X_{AC} + 13X_{BCD} + 11X_{ABCD} + 8X_{AB} \\ & - 7.5X_{CD} - 6.5X_{BD} - 6X_C - 5.5X_A + 3.75X_B \end{aligned} \tag{12}$$

The above model equation (12) is valid in the regions such as (a) $10 \leqslant X_A \leqslant 15$(cm), (b) $0.10 \leqslant X_B \leqslant 0.15$(ml h^{-1}), (c) $10 \leqslant X_C \leqslant 15$(KV), and (d) $65 \leqslant X_D \leqslant 70$(cP).

The plot of the variation in average diameters of nanofibers versus the runs (also known as the time series plot of average diameters) for a random correlation is shown in figure 7(a) as per the values listed in table 2 for all sixteen iterations. The main effects and interactions plots for the means of the average diameters (nm) with respect to the critical process parameters were plotted using MINITAB 17 software, as shown in figure 7(b) and (c). They show that *ABC*-Interaction between distance (cm), flow rate (ml h^{-1}) and voltage (KV), *AD*-Interaction between distance (cm) and viscosity (cP), *D*-Viscosity (cP), *BC*-Interaction between flow rate (ml h^{-1}) and voltage (KV), *AC*-Interaction between distance (cm) and voltage (KV), *BCD*-Interaction between flow rate (ml h^{-1}), voltage (KV) and viscosity (cP), *ABCD*-Interaction between distance (cm), flow rate (ml h^{-1}), voltage (KV) and viscosity (cP), *AB*-Interaction between distance (cm) and flow rate (ml h^{-1}), *CD*-Interaction between voltage (KV) and viscosity (cP), *BD*-Interaction between flow rate (ml h^{-1}) and viscosity (cP), *C*-Voltage (KV), *A*-Distance (cm), and *B*-Flow rate (ml h^{-1}) have the significant impact over preparation of minimum diameter of curcumin/gelatin nanofibers, as shown in table 4, figures 7(b) and (c).

The variations in diameters of nanofibers with respect to all four critical process parameters are shown in figure 7(b). It was found that with an increase in distance and voltage, the diameter of nanofibers was reduced. However, with an increase in flow rate and viscosity, the diameter of nanofibers was increased. A good interaction among all the four critical process parameters occurred is shown in figure 7(c). The effects of the contribution of *ABC*-Interaction between distance (cm), flow rate (ml h^{-1}) and voltage (KV), *AD*-Interaction between distance (cm) and viscosity (cP), *D*-Viscosity (cP), *BC*-Interaction between flow rate (ml h^{-1}) and voltage (KV), and *AC*-Interaction between distance (cm) and voltage (KV) were found to be considerable (table 4 and figure 7(c)).

The response contour lines maps of the average diameters (nm) of curcumin/gelatin nanofibers as a function of the critical process parameters are shown in figures 7(d), (f), (h), (j), (l), and (n) to define the relationships between two variables and a response. The predicted 3D response surface plots of the average diameters (nm) of curcumin/gelatin nanofibers produced by the fitted model, are shown in figures 7(e), (g), (i), (k), (m), and (o). The darkest shade in contour plots represents locations where the diameters of the nanofibers, was maximum ($>$ 280 nm) and the lightest shade represents locations where the diameters of the nanofiber was minimum ($<$ 240 nm).

It was clear after the ANOVA calculations (final ANOVA, table 4), that the factor *ACD*-Interaction between distance (cm), voltage (KV) and viscosity (cP) had the least contribution (in producing minimum diameters of curcumin/gelatin nanofibers because of the fact that it was coming as an error in DOE analysis. The effects of the contribution of *ABC*-Interaction between distance (cm), flow rate (ml h^{-1}) and voltage (KV), *AD*-Interaction between distance (cm) and viscosity (cP), *D*-Viscosity (cP), *BC*-Interaction between flow rate (ml h^{-1}) and voltage (KV), and *AC*-Interaction between distance (cm) and voltage (KV) had the considerable impacts of 24%, 16%, 15.5%, 12%, and 11.5% respectively, over the preparation of the minimum diameters of the curcumin/gelatin nanofiber.

The optimized parameter settings are shown in figure 7(p). The impacts of the critical process parameters on the average diameters (nm) of curcumin/gelatin nanofibers could be estimated by shifting the red lines to find optimal values of process parameters within the range. In our case the composite desirability, D, is 0.8129, which is close to 1. The horizontal blue line represents the current response values (figure 7(p)). The average diameter of ultrathin curcumin/gelatin nanofibers was predicted around 189.6563 nm using the optimized setting of a solution having 1.5% gelatin, 1% curcumin in 10 ml of 98% concentrated formic acid, with the electrospining unit having a voltage of 10 KV, distance from the spinneret to collector drum of 15 cm, flow rate of 0.1 ml h^{-1}, viscosity of 65 cP and drum collector speed of 1000 rpm. The figure 6(c) shows the SEM image of the curcumin/gelatin nanofibers having a 181 nm (181 $\pm$ 66 nm) average diameter, prepared under similar condition using the same solution. Thus, the estimated diameter (nm) of curcumin/gelatin nanofibers in the optimization process only has an 8% difference with the prepared diameter which shows the efficacy of present investigation.

We suggest these light weights, and ultrathin nanofibers having enough film porosity could be used in wound dressing applications due to their high surface area to volume ratio with respect to length and diameter. Researchers have been optimizing the input parameters to prepare minimum diameters of curcumin based nanofibers for various biomedical applications for the last 12 years as shown in figure 8 and table 5. In the present investigation, the optimum conditions were achieved to synthesize the minimum average diameter (181 $\pm$ 66 nm) of ultrathin curcumin/gelatin nanofibers so far which could be suitable for dressing diabetic chronic ulcers due to its unique properties such as light weight, nontoxic, biocompatible as well as water absorbent and fluid affinity.

Sharjeel *et al* [100] were successful in electrospinning a novel and hybrid polymeric nanofibrous meshes for dressing the burn wounds after incorporating gabapentin (a neuropathic pain killer) into polyethylene nanofibers and acetaminophen (a class of analgesics) into sodium alginate nanofibers, using the optimized setting of a polymeric solution of the polyethylene oxide and sodium alginate mixed in 80:20 blend proportion. The hybrid mechanism could be a safe choice in wound dressing applications. Sharjeel *et al* [101] used acetic acid

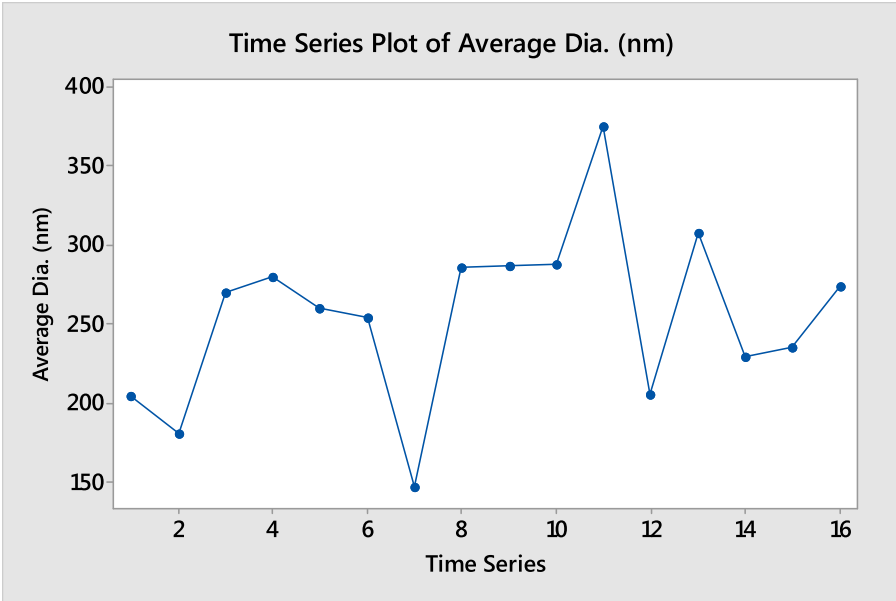

(a)

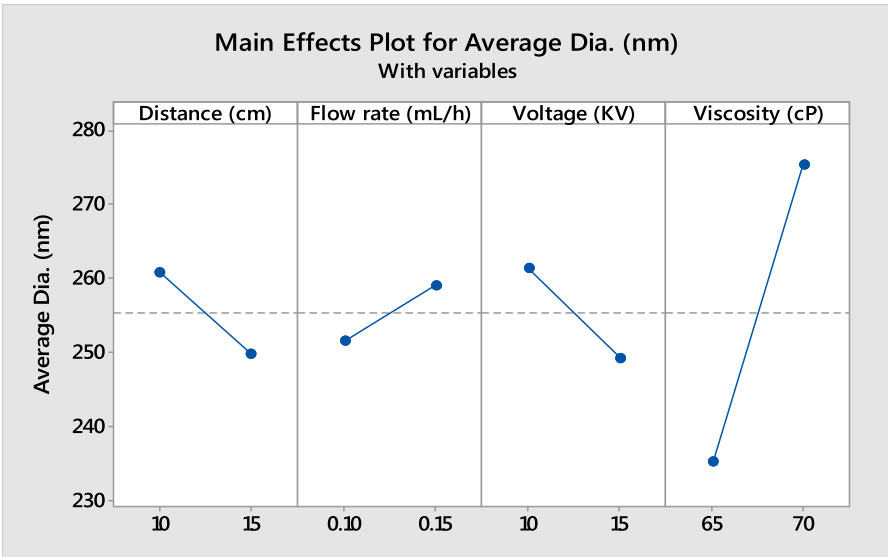

(b)

Figure 7. The process optimization of the electrospun curcumin/gelatin nanofibers. (a) The plot of the variation in average diameters of nanofibers versus the runs (also known as the time series plot of average diameters). (b) The variation in average diameters (nm) of curcumin/gelatin nanofibers with respect to the critical parameters. (c) The interaction plot to demonstrate effects of the critical process parameters on the average diameter (nm) of curcumin/gelatin nanofibers. The response contour plots of the average diameters (nm) of curcumin/gelatin nanofibers as a function of (d) distance (cm) and flow rate (ml h^{-1}) at an applied voltage of 12.5 KV and at a viscosity of 67.5 cP, (f) distance (cm) and voltage (KV) at a flow rate of 0.125 ml h^{-1} and a viscosity of 67.5 cP, (h) distance (cm) and viscosity (cP) at a flow rate of 0.125 ml h^{-1} and at an applied voltage of 12.5 KV, (j) flow rate (ml h^{-1}) and voltage (KV) at a distance of 12.5 cm from the spinneret to collector drum and a viscosity of 67.5 cP, (l) flow rate (ml h^{-1}) and viscosity (cP) at a distance of 12.5 cm from the spinneret to collector drum and at an applied voltage of 12.5 KV, and (n) voltage (KV) and viscosity (cP) at a distance of 12.5 cm from the spinneret to collector drum and a flow rate of 0.125 ml h^{-1}. The 3D response surface plots of the average diameters (nm) of curcumin/gelatin nanofibers as a function of (e) distance (cm) and flow rate (ml h^{-1}) at an applied voltage of 12.5 KV and at a viscosity of 67.5 cP, (g) distance (cm) and voltage (KV) at a flow rate of 0.125 ml h^{-1} and a viscosity of 67.5 cP, (i) distance (cm) and viscosity (cP) at a flow rate of 0.125 ml h^{-1} and at an applied voltage of 12.5 KV, (k) flow rate (ml h^{-1}) and voltage (KV) at a distance of 12.5 cm from the spinneret to collector drum and a viscosity of 67.5 cP, (m) flow rate (ml h^{-1}) and viscosity (cP) at a distance of 12.5 cm from the spinneret to collector drum and at an applied voltage of 12.5 KV, and (o) voltage (KV) and viscosity (cP) at a distance of 12.5 cm from the spinneret to collector drum and a flow rate of 0.125 ml h^{-1}. (p) The optimized responses for the minimum average diameter (nm) of curcumin/gelatine nanofibers.

and water (50:50, v/v) while preparing the solvent for synthesizing electrospun polyethylene oxide and chitosan (each dissolved separately in acetic acid and water solution in 5% weight-to-volume ratio) nanofibers (the ratio of polyethylene oxide and chitosan in the polymeric solution was 80:20). The authors incorporated nanoparticles of zinc oxide and ciprofloxacin drugs into electrospun polyethylene oxide-chitosan nanofibers

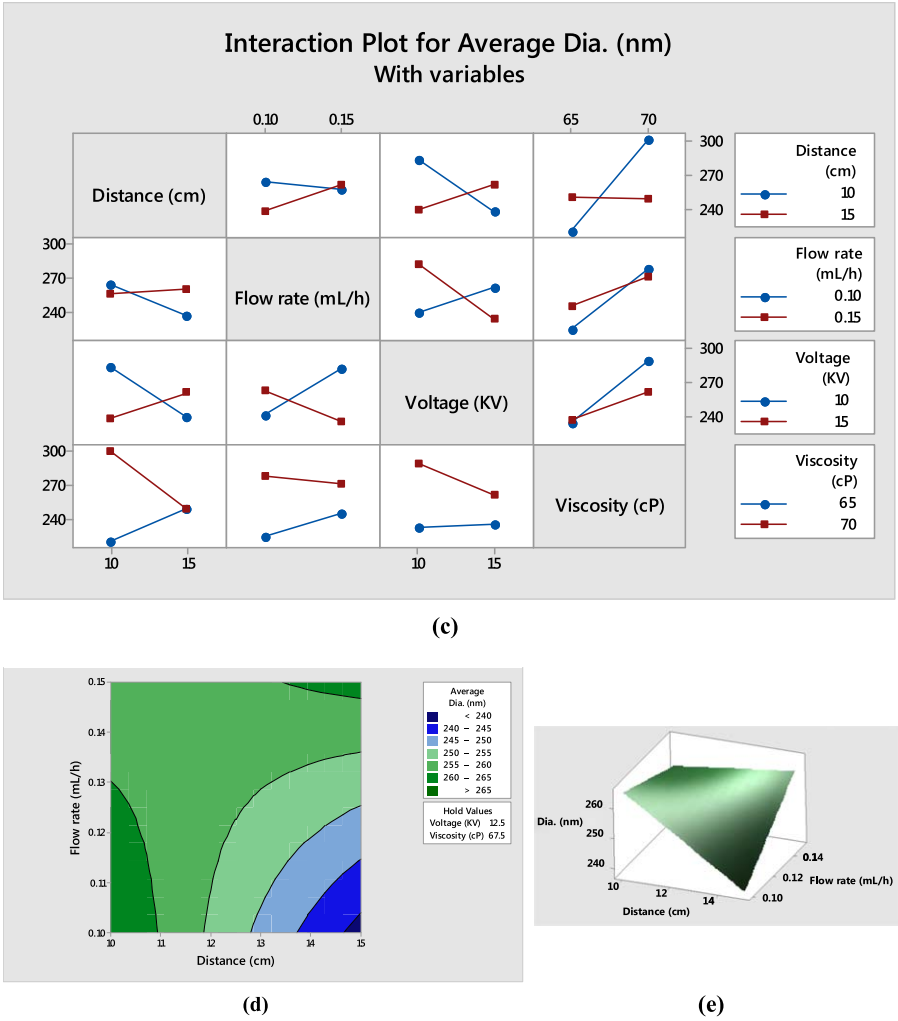

Figure 7. (Continued.)

and evaluated these drug delivery meshes as effective antibacterial systems. The authors were successful in optimizing electrospun polyethylene oxide-chitosan nanofibers of 116 nm diameters (with standard deviation of only 21 nm) using response surface methodology. They also observed that (a) a higher distance yielded lower diameters, (b) a higher voltage resulted in lower diameters, (c) with an increase in flow rate, the diameters of the nanofibers were increased, and (d) with an increase in concentration of zinc oxide nanoparticles and ciprofloxacin, the diameters of the nanofibers were increased from 116 to 210 nm and enhanced the antibacterial efficiency.

4. Future research

The application of curcumin loaded nanofibers still needs to be explored for efficient drug release during various stages of wound healing as it is still a challenge. On the basis of types of drugs to be released and various stages of wound healing, specific polymers for electrospun curcumin nanofibers have to be selected. However, the use of cytotoxic chemicals may spoil the recent research outputs in pharmaceutical applications, particularly during wound dressing. Recent studies of curcumin in nanofibers reveal a new field of research to synthesize potential biomaterials for applications in bone tissue engineering [22], treatment of diabetic chronic ulcers [20], cancers [102, 103] etc.

5. Conclusions

Our review of curcumin based, electrospun nanofibers encompassed all aspects, including the importance and need of the biofunctional nanofibers as well as the nanofibrous mats in wound healing, cancer treatment, tissue

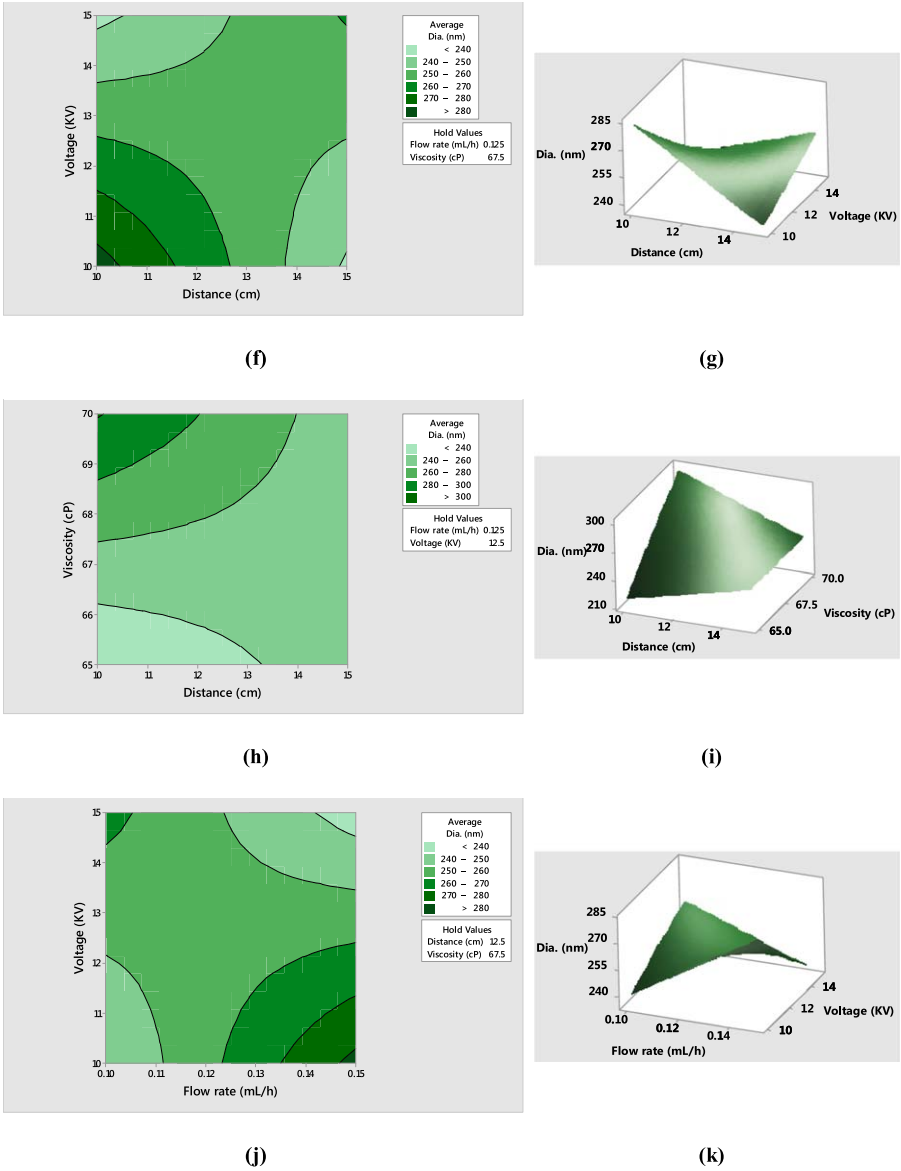

Figure 7. (Continued.)

engineering, etc to motivate researchers who are desirous to work in this innovative field of research to solve various biomedical issues using biofunctional nanofibers. The electrospinning mechanism (numerical investigations of the mechanism) was reviewed in depth in the first section of article to have better control over preparation of ultrathin curcumin/gelatin nanofibers.

In the present investigation, the mechanism behind electrospinning was discussed as used to prepare curcumin/gelatin nanofibers which would have applications in wound dressing. Gelatin was selected as the fiber material due to its nontoxic and biocompatible nature as well as it being water absorbent (fluid affinity), thus supporting moist wound healing in further applications. Gelatin is commercially available at relatively low cost and thus was the obvious choice in the present investigation. Using electrospining, light weight, ultrathin, and porous nanofibers having average diameters of 147 nm (147 $\pm$ 34 nm) were prepared successfully at a higher voltage, such as 15 KV (at 10 cm distance, 0.15 ml h^{-1} flow rate, 65 cP viscosity and drum collector speed of 1000 rpm) using the solution having 1.5% gelatin, and 1% curcumin in 10 ml of 98% concentrated formic acid (figure 6(d) and table 2).

After determining the relative effects of the various spinning factors, as shown in table (table 4), we arrived at the following conclusions: (a) *ABC*-Interaction between distance (cm), flow rate (ml h^{-1}) and voltage (KV), *AD*-Interaction between distance (cm) and viscosity (cP), *D*-Viscosity (cP), *BC*-Interaction between flow rate (ml h^{-1}) and voltage (KV), and *AC*-Interaction between distance (cm) and voltage (KV) have the considerable impacts of 24%, 16%, 15.5%, 12%, and 11.5% respectively, over the preparation of the minimum diameters of

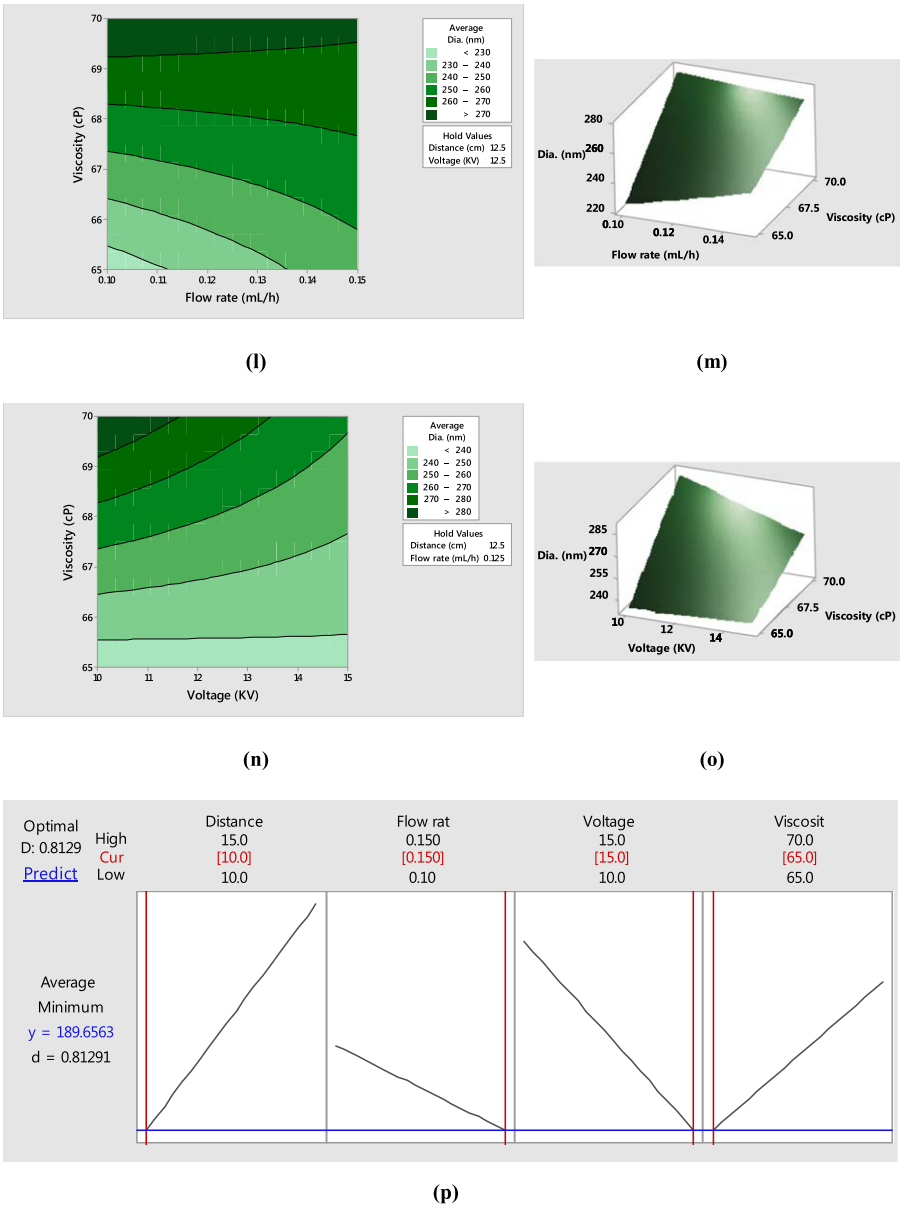

Figure 7. (Continued.)

the curcumin/gelatin nanofiber, (b) *BCD*-Interaction between flow rate (ml h^{-1}), voltage (KV) and viscosity (cP), *ABCD*-Interaction between distance (cm), flow rate (ml h^{-1}), voltage (KV) and viscosity (cP), *AB*-Interaction between distance (cm) and flow rate (ml h^{-1}), CD-Interaction between voltage (KV) and viscosity (cP), *BD*-Interaction between flow rate (ml h^{-1}) and viscosity (cP), *C*-Voltage (KV), *A*-Distance (cm), and *B*-Flow rate (ml h^{-1}) have the significant impact over preparation of minimum diameter of curcumin/gelatin nanofibers, and (c) *ACD*-Interaction between distance (cm), voltage (KV) and viscosity (cP) affects the diameter (nm) by *0.05%* only which is not significant.

The 2^k factorial design of experiment was used as an efficient technique to empirically examine the effects of all four critical process parameters on the diameter of the nanofibers. MINITAB *17* software was used for plotting graphs for study of the variation in diameters of nanofibers with respect to input parameters. The variation in diameters of nanofibers with respect to the critical process parameters that were observed include (a) a higher distance yielded lower diameters, (b) a higher voltage resulted in lower diameters, (c) with an increase in flow rate, the diameters of the nanofibers were increased, and (d) with an increase in viscosity, the diameters of the nanofibers were increased.

The optimum condition for the development of ultrathin curcumin/gelatin nanofibers having a 189.6563 nm average diameter was estimated using the optimized setting of a solution having 1.5% gelatin, 1% curcumin in 10 ml of 98% concentrated formic acid, with the electrospining unit having a voltage of 15 KV,

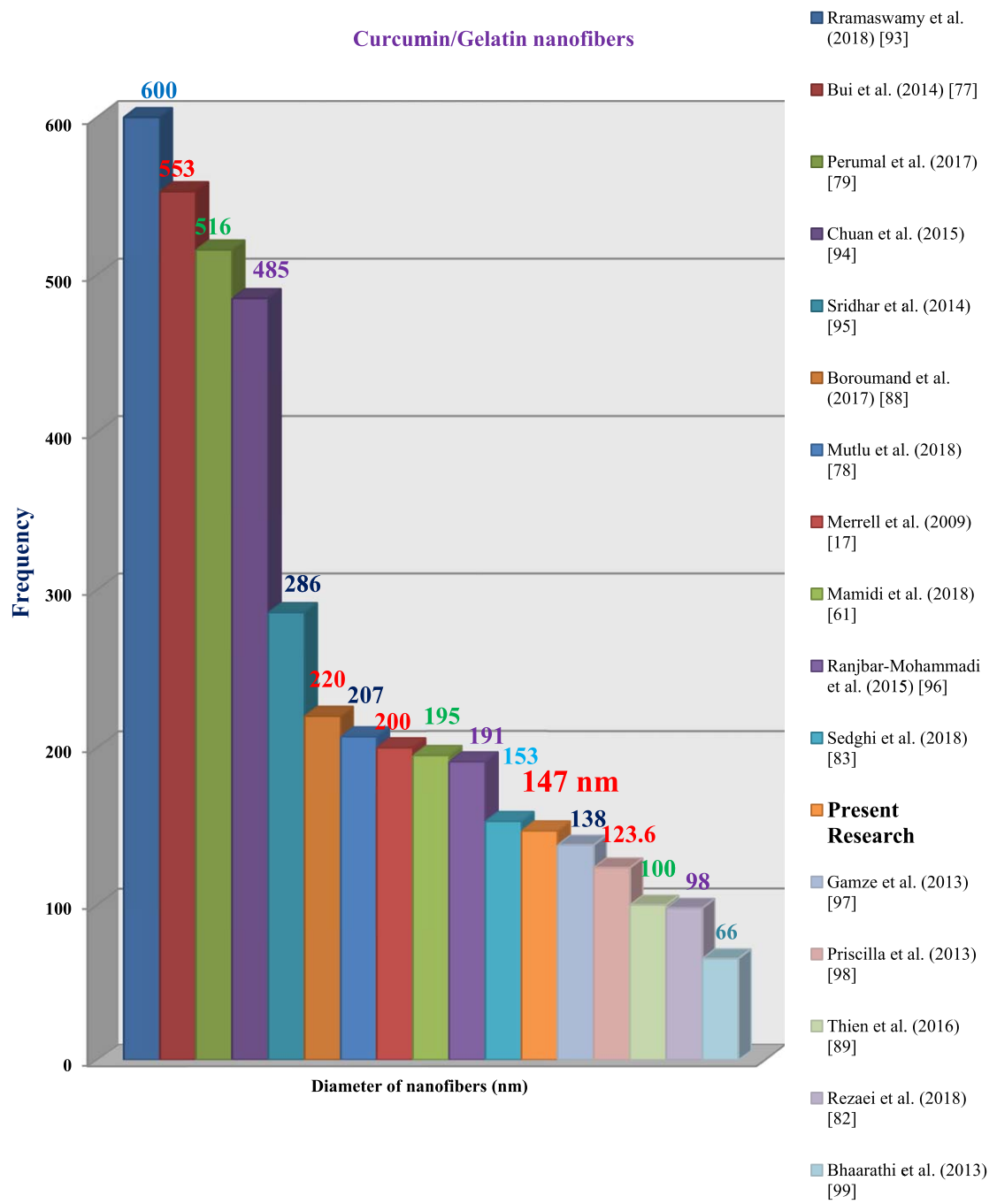

Figure 8. Synthesis of lowest diameter of curcumin /gelatin nanofibers.

distance from the spinneret to collector drum of 15 cm, flow rate of 0.1 ml h^{-1}, viscosity of 65 cP and drum collector speed of 1000 rpm. The estimated average diameter (nm) of curcumin/gelatin nanofibers in the optimization process only has an 8% difference with the prepared average diameter, i.e., 181 nm (181 $\pm$ 66 nm), which shows the efficacy of the present investigation.

These ultrathin nanofibers having enough film porosity were biocompatible, nontoxic as well as biodegradable in nature and thus it is suggested that they could be used in dressing problematic wounds, such as diabetic chronic ulcers, as these have unique properties, such as high surface area to volume ratio and light weight, for sustained release of curcumin during healing. This research paper presented so far is very different from its kind as it encompasses (a) the entire electrospinning mechanism (numerical investigations of the mechanism) to have better control over preparation of ultrathin nanofibers, and (b) the applications of the nanofibrous mats (incorporating biofunctional nanofibers) which are in use now-a-days, after reviewing sufficient number of papers prior to actual optimization for the lowest diameter range using theoretical analysis

Table 5. Recent achievements in optimization of curcumin based electrospun nanofibers.

Researchers	Average diameters of nanofibers (nm)	Details of nanofibers
Rramaswamy *et al* (2018) [93]	600 (± 50)	Tetrahydro curcumin (THC) loaded poly (vinyl pyrrolidone) (PVP) nanofibers
Bui *et al* (2014) [17]	553	Curcumin contatining polycaprolactone (PCL) nanofibers
Perumal *et al* (2017) [19]	516	Poly (lactic acid)/curcumin nanofibers
Chuan *et al* (2015) [94]	485 (± 123)	Curcumin loaded polyvinyl pyrrolidone (PVP) nanofibers
Sridhar *et al* (2014) [95]	286 (± 90)	Curcumin loaded PCL/aloe vera nanofibers
Boroumand *et al* (2017) [28]	220 (± 100)	Curcumin contatining polycaprolactone (PCL) nanofibers
Mutlu *et al* (2018) [18]	207 (± 56)	Curcumin loaded poly (3-hydroxy butyric acid-co-3-hydroxy valeric acid) (PHBV) nanofibers
Merrell *et al* (2009) [30]	200	Curcumin loaded poly(ε-caprolactone) nanofibers
Mamidi *et al* (2018) [74]	195 (± 200)	Curcumin embedded gelatin-polylactic acid nanofibers
Ranjbar-Mohammadi *et al* (2015) [96]	191(± 24)	Curcumin loaded poly(ε-caprolactone)/gum tragacanth nanofibers
Sedghi *et al* (2018) [23]	153 (± 31)	Zinc-curcumin loaded coaxial nanofibers
Present research	147 (± 34)	Curcumin/gelatin nanofibers
Gamze *et al* (2013) [97]	138 (± 39)	Curcumin loaded polyethylene oxide (PEO)/hydroxypropyl methylcellulose (HPMC) nanofibers
Priscilla *et al* (2013) [98]	123.6 (± 26.8)	Poly(lactic-co-glycolic acid)/curcumin nanofibers
Thien *et al* (2016) [29]	100	Curcumin loaded chitosan/poly (vinyl alcohol) PVA nanofibers
Rezaei *et al* (2018) [22]	98 (± 18)	Curcumin loaded almond gum nanofibers
Bhaarathi *et al* (2013) [99]	66.81	Curcumin loaded chitosan/poly (lactic acid) nanofibers

(which are validated too using experimental results). Finally, the optimized settings (to obtain ultrathin nanofibers) were proposed for the electrospinning process parameters to prepare nanofibers mats for biomedical applications, such as wound healing (through sustained release of curcumin during crucial hours of healing).

Conflicts of interest

The authors declare that there are no conflicts of interest.

Additional information

Nand Jee Kanu, Research Scholar, S. V. National Institute of Technology, Surat, India; Eva Gupta, Research Scholar, Amity University, Uttar Pradesh, India; Umesh Kumar Vates, Associate Professor, Amity University, Uttar Pradesh, India; and Gyanendra Kumar Singh, Faculty, Adama Science and Technology University, Adama, Ethiopia; have not been funded in any way to carry out the research activities.

Author(s) contributions statements

Author(s) contribution in the manuscript entitled 'Electrospinning Process Parameters Optimization for Biofunctional Curcumin/Gelatin Nanofibers' is as follows:

Nand Jee Kanu is a Research Scholar in S. V. National Institute of Technology, Surat, India. He is pursuing a PhD in Mechanical Engineering. He has critically reviewed the applications of electrospun curcumin/gelatin nanofibers in wound healing and done further investigations for achieving minimum diameters range of nanofibers to compile the entire research work.

Eva Gupta is a Research Scholar in Amity University, Uttar Pradesh, India. She is pursuing PhD in Electrical Engineering. She has reviewed papers on electrospinning and done numerical investigations for optimization of process parameters for minimum average diameters of curcumin/gelatin nanofibers.

Umesh Kumar Vates is Associate Professor in Mechanical Engineering Department in Amity University, Uttar Pradesh, India. He has completed his PhD in Mechanical engineering from IIT Dhanbad (An Institute of National Importance). His role is as expert in this work while monitoring and motivating the above PhD students. He has developed the optimization technique which has been implemented in this research work.

Gyanendra Kumar Singh is Faculty in Manufacturing Engineering Department in Adama Science and Technology University, Adama, Ethiopia. He has completed his PhD in Mechanical engineering from NIT Allahabad (An Institute of National Importance). His role is as expert in this work while monitoring and motivating above PhD students. He has suggested suitable optimization technique to successfully compile the research work.

ORCID iDs

Nand Jee Kanu https://orcid.org/0000-0003-3919-5098
Eva Gupta https://orcid.org/0000-0002-6388-7791
Umesh Kumar Vates https://orcid.org/0000-0002-1614-5082
Gyanendra Kumar Singh https://orcid.org/0000-0003-3765-9071

References

[1] Khajavi R and Abbasipour M 2012 Electrospinning as a versatile method for fabricating core–shell, hollow and porous nanofibers *Scientia Iranica F.* **19** 2029–34
[2] Skinner J L, Andriolo J M, Murphy J P and Ross B M 2017 Electrospinning for nano- to mesoscale photonic structures *Nanophotonics.* **6** 765–87
[3] Huang Z-X, Wu J-W, Wong S-C, Qu J-P and Srivatsan T S 2017 The technique of electrospinning for manufacturing core–shell nanofibers *Mater. Manuf. Processes* (https://doi.org/10.1080/10426914.2017.1303144)
[4] Ramakrishna S, Fujihara K, Teo W-E, Yong T, Zuwei M and Ramakrishna R 2006 Electrospun nanofibers: solving global issues *Mater. Today* **9** 40–50
[5] Pengcheng L, Yanbo L, Jinbo and Yao. A 2010 Review on the research status of massive production of nanofibers via electrospinning technology *Proc. of the Int. Conf. on Information Technology and Scientific Management, Scientific Research* 326–8
[6] Reneker D H and Chun I 1996 Nanometer diameter fibers of polymer, produced by electrospinning *Nanotechnology* **7** 216–23
[7] Jamil A M, Gary E W, David G S and Gary L B 2002 Electrospinning of collagen nanofibers *Biomacromolecules.* **3** 232–8
[8] Pham Q P, Sharma U and Mikos A G 2006 Electrospinning of polymeric nanofibers for tissue engineering applications: a review *Tissue Eng.* **12** 1197–211
[9] Vasita R and Katti D S 2006 Nanofibers and their applications in tissue Engineering *Int. J. Nanomed.* **1** 15–30
[10] Kriegel C, Arrechi A, Kit K, McClements D J and Jochen W 2008 Fabrication, functionalization, and application of electrospun biopolymer nanofibers *Crit. Rev. Food Sci. Nutr.* **48** 775–97
[11] Shekh R, Princeton C and Narayan B 2017 Aloe vera for tissue engineering applications *J. Funct. Biomater.* 8
[12] Tuerdimaimaiti A, Adnan M, Halimatu M, Kasturi J N, Thibault C and Sidi A B 2019 Latest progress in electrospun nanofibers for wound healing applications *ACS Appl. Bio Mater.* (https://doi.org/10.1021/acsabm.8b00637)
[13] Amariei G, Kokol V, Boltes K and Letón P 2018 Incorporation of antimicrobial peptides on electrospun nanofibres for biomedical applications *RSC Adv.* **8** 2801328023
[14] Yoon J, Yang H-S, Lee B-S and Yu W-R 2018 Recent progress in coaxial electrospinning: new parameters, various structures, and wide applications *Adv. Mater.* **30** 1704765
[15] Alharbi H F, Luqman M, Khalil A, Elnakady Y A, Eikader O A, Rady A, Alharthi A H and Karim M R 2018 Fabrication of core–shell structured nanofibers of poly (Lactic Acid) and poly (Vinyl Alcohol) by coaxial electrospinning for tissue engineering *Eur. Polym. J.* **98** 483–91
[16] Chen S, Liu B, Carison M A, Gombart A F, Reilly D A and Xie J 2017 Recent Advances in electrospun nanofibers for wound healing *Nanomedicine (Lond).* **12** 1335–52
[17] Bui H T, Chung O H, Cruz J D and Park J S 2014 Fabrication and characterization of electrospun curcumin-loaded polycaprolactone-polyethylene glycol nanofibers for enhanced wound healing *Macromol. Res.* **22** 1288–96
[18] Mutlu G, Calamak S, Ulubayram K and Guven E 2018 Curcumin-loaded electrospun PHBV nanofibers as potential wound-dressing material *J. Drug Deliv. Sci. Technol.* **43** 185–93
[19] Perumal G, Pappuru S, Chakraborty D, Nandkumar A M, Chand D K and Doble M 2017 Synthesis and characterization of curcumin loaded PLA-Hyperbranched polyglycerol electrospun blend for wound dressing applications *Materials Science and Engineering* C **76** 1196–204
[20] Seyed M S, Hamid M, Mojgan Z and Jalal B 2017 Designing and fabrication of curcumin loaded PCL/PVA multilayer nanofibrous electrospun structures as active wound dressing *Prog Biomater.* **6** 39–48
[21] Ranjbar-Mohammadi M, Rabbani S, Bahrami S H, Joghataei M T and Moayer F 2016 Antibacterial performance and *in vivo* diabetic wound healing of curcumin loaded gum tragacanth/poly(ε-caprolactone) electrospun nanofibers *Materials Science and Engineering* C **69** 1183–91
[22] Rezaei A and Nasirpour A 2018 Encapsulation of curcumin using electrospun almond gum nanofibers: fabrication and characterization *Int. J. Food Prop.* **21** 1608–18
[23] Sedghi R, Sayyari N, Shaabani A, Niknejad H and Tayebi T 2018 Novel biocompatible zinc-curcumin loaded coaxial nanofibers for bone tissue engineering application *Polymer* (https://doi.org/10.1016/j.polymer.2018.03.045)
[24] Wang H, Hao L, Wang P, Chen M, Jiang S and Jiang S 2017 Release kinetics and antibacterial activity of curcumin loaded zein fibers *Food Hydrocolloids* **63** 437–46
[25] Tsekova P B, Spasova M G, Manolova N E, Markova N D and Rashkov I B 2017 Electrospun curcumin-loaded cellulose acetate/polyvinylpyrrolidone fibrous materials with complex architecture and antibacterial activity *Materials Science and Engineering* C **73** 206–14
[26] Shababdoust A, Ehsani M, Shokrollahi P and Zandi M 2017 Fabrication of curcumin-loaded electrospun nanofiberous polyurethanes with anti-bacterial activity *Progress in Biomaterials.* (https://doi.org/10.1007/s40204-017-0079-5)
[27] Deng L, Kang X, Liu Y, Feng F and Zhang H 2017 Effects of surfactants on the formation of gelatin nanofibers for controlled release of curcumin *Food Chem.* (https://doi.org/10.1016/j.foodchem.2017.03.027)

[28] Boroumand S, Hosseini S, Salehi M and Faridi-Majidi R 2017 Drug-loaded electrospun nanofibrous sheets as barriers against postsurgical adhesions in mice model *Nanomed Res J.* **2** 64–72
[29] Thien D V H, Quyen T T B, Tri N M, Thoa T T K and Tham N T N 2016 Electrospun chitosan/PVA nanofibers for drug delivery *J. Sci. Technol.* **54** 185–92
[30] Merrell J G, McLaughlin S W, Tie L, Laurencin C T, Alex F C and Lakshmi S N 2009 Curcumin loaded poly (ε-Caprolactone) nanofibers: diabetic wound dressing with antioxidant and anti-inflammatory properties *Clin Exp Pharmacol Physiol.* **36** 1149–56
[31] Narges F, Majid D, Jebraeel M and Azadeh S 2018 Curcumin nanofibers for the purpose of wound healing *J. Cell. Physiol.* 1–18
[32] Mouthuy P-A, Škoc M S, Gašparović A Č, Milković L, Carr A J and Zarkovic N 2017 Investigating the use of curcumin-loaded electrospun filaments for soft tissue repair applications *Int. J. Nanomed.* **12** 3977–91
[33] Xinyi D, Juan L, Huaiyuan Z, Johannes W, Ursula H, Stefanie S, Carina P, Yi S, Machens H-G and Arndt F S 2017 Nano-formulated curcumin accelerates acute wound healing through Dkk-1-mediated fibroblast mobilization and MCP-1-mediated anti-inflammation *NPG Asia Mater.* **9** e368
[34] Chang S K, Doo H B, Kyung D G, Ki H L, In C U and Young H P 2005 Characterization of gelatin nanofiber prepared from gelatin-formic acid solution *Polymer* **46** 5094–102
[35] Deng L, Kang X, Liu Y, Feng F and Hui Z 2018 Characterization of gelatin/zein films fabricated by electrospinning versus solvent casting *Food Hydrocoll.* **74** 324–32
[36] Sadaf S G, Sima H and Hosein N 2018 Fabrication and characterization of chitosan/gelatin/thermoplastic polyurethane blend nanofibers *Journal of Textiles and Fibrous Materials.* **1** 1–8
[37] Ditpon K, Masaharu H, Mayuko O, Satoshi U, Masashi I, Tetsuya F and Hiroshi T 2019 Preparation and characterization of electrospun gelatin nanofibers for use as nonaqueous electrolyte in electric double-layer capacitor *Journal of Nanotechnology.* (https://doi.org/10.1155/2019/2501039)
[38] Lin L, Gu Y and Cui H 2018 Novel electrospun gelatin-glycerin-ε-poly-lysine nanofibers for controlling *Listeria monocytogenes* on beef *Food Packaging and Shelf Life.* **18** 21–30
[39] Bazbouz M B, Liang H and Tronci G 2018 A UV-cured nanofibrous membrane of vinylbenzylated gelatin-poly (ε-caprolactone) dimethacrylate co-network by scalable free surface electrospinning *Materials Science and Engineering* C **91** 541–55
[40] Yabing W, Haoxuan L, Yanhuizhi F, Peilin J, Jiansheng S and Chen H 2019 Dual micelles-loaded gelatin nanofibers and their application in lipopolysaccharide-induced periodontal disease *Int. J. Nanomed.* **14** 963–76
[41] Jang H J, Kim Y M, Yoo B Y and Seo Y K 2018 Wound-healing effects of human dermal components with gelatin dressing *J. Biomater. Appl.* **32** 716–24
[42] Aytac Z, Ipek S, Erol I, Durgun E and Tamer U 2019 Fast-dissolving electrospun gelatin nanofibers encapsulating ciprofloxacin/cyclodextrin inclusion complex *Colloids Surf. B Biointerfaces.* **178** 129–36
[43] Piran M, Shiri M, Soufi Z M, Esmaeili E, Soufi Z M, Vazifeh S N, Mahboudi H, Daneshpazhouh H, Dehghani N and Hosseinzadeh S 2019 Electrospun triple-layered PLLA/gelatin. PRGF/PLLA scaffold induces fibroblast migration *J. Cell. Biochem.* 1–13
[44] Novickij V, Švedienė J, Paškevičius A, Markovskaja S, Girkontaitė I, Zinkevičienė A, Lastauskienė E and Novickij J 2018 Pulsed electric field-assisted sensitization of multidrug-resistant Candida albicans to antifungal drugs *Future Microbiol.* **13** 535–46
[45] Christina K, Alessandra A, Kevin K, McClements D J and Weiss J 2008 Fabrication, functionalization, and application of electrospun biopolymer nanofibers *Crit. Rev. Food Sci. Nutr.* **48** 775–97
[46] Liu X, Nielsen L H, Klodzinska S N, Nielsen H M, Qu H, Christensen L P, Rantanen J and Yang M 2018 Ciprofloxacin-loaded sodium alginate/poly (Lactic-Co-Glycolic Acid) electrospun fibrous mats for wound healing *Eur. J. Pharm. Biopharm.* **123** 42–9
[47] Chouhan D, Janani G, Chakraborty B, Nandi S K and Mandal B B 2018 Functionalized PVA-silk blended nanofibrous mats promote diabetic wound healing via regulation of extracellular matrix and tissue remodelling *J. Tissue Eng. Regen. Med.* **12** e1559–70
[48] Gizaw M, Thompson J, Faglie A and Lee S Y 2018 Electrospun fibers as a dressing material for drug and biological agent delivery in wound healing applications *Bioengineering.* **5** 1–33
[49] Tonda-Turo C, Ruini F, Ceresa C, Gentile P, Varela P, Ferreira A M, Fracchia L and Ciardelli G 2018 Nanostructured scaffold with biomimetic and antibacterial properties for wound healing produced by 'green electrospinning approach *Colloids Surf. B* **1** 1–34
[50] Mindru T B, Mindru I B, Malutana T and Turab V 2007 Electrospinning of high concentration gelatin solutions *J. Optoelectron. Adv. Mater.* **9** 3633–8
[51] Maleknia L and Majdi Z R 2014 Electrospinning of gelatin nanofiber for biomedical application *Orient. J. Chem.* **30** 2043–8
[52] Chen H-C, Jao W-C and Yang M-C 2008 Characterization of gelatin nanofibers electrospun using ethanol/formic acid/water as a solvent *Polymer Advanced Technologies.* **20** 98–103
[53] Vitalij N, Eglė L, Gediminas S, Irutė G, Auksė Z, Jurgita Š, Algimantas P, Svetlana M and Jurij N 2019 Low concentrations of acetic and formic acids enhance the inactivation of *Staphylococcus aureus* and Pseudomonas aeruginosa with pulsed electric fields *BMC Microbiol.* 19
[54] Constantin T, Konstantinos D, Zacharias D S, Sophia H, Han Z, Liu Z L, Wyche J H and Pantazis P 2007 Metabolism and anticancer activity of the curcumin analogue, dimethoxycurcumin *Clin Cancer Res.* **13** 1269–77
[55] Ramírezagudelo R, Scheuermann K, Galagarcía A, Monteiro A, Pinzón-García A D, Cortés M E and Sinisterra R D 2018 Hybrid nanofibers based on poly-caprolactone/gelatin/hydroxyapatite nanoparticles-loaded doxycycline: effective anti-tumoral and antibacterial activity *Materials Science and Engineering* C **83** 25–34
[56] Wong K, Ngai S, Lee L, Goh B, Chan K-G and Chuah L-H 2018 Curcumin nanoformulations for colorectal cancer: a review *Front. Pharmacol.* **10** 152
[57] Chen Y, Du Q, Guo Q, Huang J, Liu L, Shen X and Peng J 2018 A W/O emulsion mediated film dispersion method for curcumin encapsulated pH-sensitive liposomes in the colon tumor treatment *Drug Dev. Ind. Pharm.* 1–10
[58] Ferri C, West K, Otero K and Kim Y H 2018 Effectiveness of curcumin for treating cancer during chemotherapy *Altern Complement Ther.* **24** 13–8
[59] Javadi S, Rostamizadeh K, Hejazi J, Parsa M and Fathi M 2018 Curcumin mediated down-regulation of alphaV beta3 integrin and up-regulation of pyruvate dehydrogenase kinase 4 (PDK4) in Erlotinib resistant SW480 colon cancer cells *Phytother Res.* **32** 355–64
[60] Marjaneh R M *et al* Phytosomal curcumin inhibits tumor growth in colitis-associated colorectal cancer *J. Cell. Physiol.* 2018 **233** 6785–98
[61] Sesarman A, Tefas L, Sylvester B, Licarete E, Rauca V, Luput L, Patras L, Banciu M and Porfire A 2018 Anti-angiogenic and anti-inflammatory effects of long-circulating liposomes co-encapsulating curcumin and doxorubicin on C26 murine colon cancer cells *Pharmacol Rep.* **70** 331–9
[62] Enas A, Clive J R, Rozita R, Kah H Y and Eng K S 2018 Pharmacokinetic and anti-colon cancer properties of curcumin-containing chitosan-pectinate composite nanoparticles *J. Biomater. Sci., Polym. Ed.* (https://doi.org/10.1080/09205063.2018.1541500)

[63] Yasmine A *et al* Live single cell mass spectrometry reveals cancer-specific metabolic profiles of circulating tumor cells *Cancer Sci.* 2019 **110** 697–706
[64] Rafael C-C, Laura C, Gloria P, Amelia D, Juan M L-R, Consolación M and Jose P 2019 Electrospun nanofibers: recent applications in drug delivery and cancer therapy *Nanomaterials.* **9** 656
[65] Feifei W, Zhaoyang S, Jing Y and Lan X 2019 Preparation, characterization and properties of porous PLA/PEG/Curcumin composite nanofibers for antibacterial application *Nanomaterials.* **9** 508
[66] Wang J and Windbergs M 2018 Influence of polymer composition and drug loading procedure on dual drug release from plga:peg electrospun fibers *Eur. J. Pharm. Sci.* **124** 71–9
[67] Negut I, Grumezescu V and Grumezescu A M 2018 Treatment strategies for infected wounds *Molecules.* **2329** 1–23
[68] Hoang M S, Doan N H and Huynh D P 2017 Fabrication of curcumin loaded nano polycaprolactone/chitosan nonwoven fabric via electrospinning technique *J. Sci. Technol.* **55** 99–108
[69] Abdollahi E, Momtazi A A, Johnston T P and Sahebkar A 2018 Therapeutic effects of curcumin in inflammatory and immune mediated diseases: a nature-made jack-of-all-trades ? *J. Cell. Physiol.* **233** 830–48
[70] Dai J, Gu L, Su Y, Wang Q, Zhao Y, Chen X, Deng H, Li W, Wang G and Li K 2018 Inhibition of curcumin on influenza A virus infection and influenzal pneumonia via oxidative stress, TLR2/4, p38/JNK MAPK and NF-κB pathways *Int. Immunopharmacol.* **54** 177–87
[71] Panahi Y, Khalili N, Sahebi E, Namazi S, Simental-Mendía L E, Majeed M and Sahebkar A 2018 Effects of curcuminoids plus piperine on glycemic, hepatic and inflammatory biomarkers in patients with type 2 diabetes mellitus: A randomized double-blind placebo-controlled trial *Drug Research.* **68** 403–9
[72] Zhao Y, Liu J G, Chen W M and Yu A X 2018 Efficacy of thermosensitive chitosan/β-glycerophosphate hydrogel loaded with βcyclodextrin-curcumin for the treatment of cutaneous wound infection in rats *Experimental and Therapeutic Medicine.* **15** 1304–13
[73] Mamidi N, Romo I L, Gutiérrez H M L, Barrera E V and Alex E-Z 2018 Development of forcespun fiber-aligned scaffolds from gelatin–zein composites for potential use in tissue engineering and drug release *MRS Commun.* 1–8
[74] Mamidi N, Romo I L, Barrera E V and Alex E-Z 2018 High throughput fabrication of curcumin embedded gelatin-polylactic acid forcespun fiber-aligned scaffolds for the controlled release of curcumin *MRS Commun.* 1–9
[75] Ravikumar R, Ganesh M, Senthil V, Ramesh Y V, Jakki S L and Eun Y C 2018 Tetrahydro curcumin loaded PCL-PEG electrospun transdermal nanofiber patch: Preparation, characterization, and *in vitro* diffusion evaluations *J. Drug Del. Sci. Tech.* **44** 342–8
[76] Weilan Y *et al* Simultaneous determination of curcumin, tetrahydrocurcumin, quercetin, and paeoniflorin by UHPLC-MS/MS in rat plasma and its application to a pharmacokinetic study *J. Pharm. Biomed. Anal.* 2019 **172** 58–66
[77] Wang Y and Xu L 2018 Preparation and characterization of porous core–shell fibers for slow release of tea polyphenols *Polymers.* **10** 144
[78] Lu H, Qiu Y, Wang Q, Li G and Qufu W 2018 Nanocomposites prepared by electrohydrodynamics and their drug release properties *Materials Science and Engineering* C **91** 26–35
[79] Zhang L, Wang Z, Xiao Y, Liu P, Shige W, Yili Z, Mingwu S and Xiangyang S 2018 Electrospun PEGylated PLGA nanofibers for drug encapsulation and release *Mater. Sci. Eng.* C **91** 255–62
[80] Mostafalu P *et al* Smart bandage for monitoring and treatment of chronic wounds *Small.* 2018 **14** 1703509
[81] Haley R M and Von R H A 2018 Localized and targeted delivery of nsaids for treatment of inflammation: a review *Exp. Biol. Med.* 1535370218787770
[82] Cheng H, Yang X, Che X, Yang M and Guangxi Z 2018 Biomedical application and controlled drug release of electrospun fibrous materials *Materials Science and Engineering* C **90** 750–63
[83] Hao S, Zhang Y, Meng J, Liu J, Wen T, Gu N and Xu H 2018 Integration of a superparamagnetic scaffold and magnetic field to enhance the wound-healing phenotype of fibroblasts *ACS Appl. Mater. Interfaces* **10** 22913–23
[84] Abudula T *et al* The effect of poly (Glycerol Sebacate) Incorporation within hybrid chitin–lignin sol–gel nanofibrous scaffolds *Materials.* 2018 **11** 451
[85] Novickij V, Zinkevičienė A, Perminaitė E, Čėsna R, Eglė L, Algimantas P, Jurgita Š, Svetlana M, Jurij N and Irutė G 2018 Noninvasive nanosecond electroporation for biocontrol of surface infections: an *in vivo* study *Sci. Rep.* **8** 14516
[86] Mi Y, Xu J, Tang X, Bian C, Hongliang L, Qiyu Y and Junying T 2018 Scaling relationship of *in vivo* muscle contraction strength of rabbits exposed to high-frequency nanosecond pulse bursts *Technol. Cancer Res. Treat.* **17** 1533033818788078
[87] Yeo Y L and Friend R J 2006 Electrospinning carbon nanotube polymer composite nanofibers *J. Exp. Nanosci.* **1** 177–209
[88] Rafiei S, Maghsoodlou S, Saberi M, Lotfi S, Motaghttalab V, Noroozi B and Haghi A K 2014 New Horizons in modeling and simulation of electrospun nanofibers: a detailed review *Cellulose Chem. Technol.* **48** 401–24
[89] Mir R M, Mehdi R and Farhad S 2015 Investigation of effect of electrospinning parameters on morphology of polyacrylonitrile/polymethyl methacrylate nanofibers: a box-behnken based study *Journal of Macromolecular Science, Part B: Physics.* (https://doi.org/10.1080/00222348.2015.1042628)
[90] Vince B and Xuejun W 2009 Effect of electrospinning parameters on the nanofiber diameter and length *Materials Science and Engineering* C **29** 663–8
[91] Montgomery D C 2013 *Design and Analysis of Experiments.* (New York: Wiley) Student Edition8th Edn
[92] Ross P J 1989 *Taguchi techniques for quality engineering.* (New York: McGraw Hill Book Company)
[93] Rramaswamy R, Mani G and Jang H T 2018 Fabrication of buccal dissolving tetrahydro curcumin loaded polyvidone fiber mat: synthesis, characterization, and *in vitro* evaluations . *Journal of Applied Pharmaceutical Science.* **8** 026–31
[94] Chuan W, Chao M, Zhenkai W, He L, Peng Y, Jia S, Nan M and Qinghua Z 2015 Enhanced bioavailability and anticancer effect of curcumin-loaded electrospun nanofiber: *in vitro* and *in vivo* study *Nanoscale Res. Lett.* 10
[95] Sridhar R *et al* Curcumin- and natural extract-loaded nanofibres for potential treatment of lung and breast cancer: *in vitro* efficacy evaluation *J. Biomater. Sci., Polym. Ed.* 2014 **25** 985–98
[96] Ranjbar-Mohammadi M and Bahrami S H 2015 Electrospun curcumin loaded poly(epsilon-caprolactone)/gum tragacanth nanofibers for biomedical application *Int. J. Biol. Macromol.* (https://doi.org/10.1016/j.ijbiomac.2015.12.024)
[97] Gamze R, Mehmet B, Serdar T and Füsun A 2013 Studies on improvement of water-solubility of curcumin with electrospun nanofibers *FABAD J. Pharm. Sci.* **38** 143–9
[98] Priscilla P L, Marcio LAe S and Juan P H 2013 Curcumin-loaded biodegradable electrospun fibers: preparation, characterization, and differences in fiber morphology *International Journal of Polymer Anal. Charact.* **18** 534–44
[99] Bhaarathi D, Nachimuthu S, Ramasamy M, Ponnusamy S, Palanisamy V, Sukumar V and Venugopal R 2013 Electrospinning of curcumin loaded chitosan/poly (lactic acid) nanofilm and evaluation of its medicinal characteristics *Front. Mater. Sci.* **7** 350–61

[100] Sharjeel A, Tanveer H, Ahsan N, Abdul Z and Nabyl K 2019 A novel double-layered polymeric nanofiber-based dressing with controlled drug delivery for pain management in burn wounds *Polym. Bull.* (https://doi.org/10.1007/s00289-019-02727-w)
[101] Sharjeel A, Tanveer H, Ahsan N, Abdul Z, Seeram R, Misbah H and Nabyl K 2019 Enhanced antibacterial activity of PEO-chitosan nanofibers with potential application in burn infection management *Int. J. Biol. Macromol.* **135** 1222–36
[102] Gang G, ShaoZhi F, LiangXue Z, Hang L, Min F, Feng L, ZhiYong Q and YuQuan W 2011 Preparation of curcumin loaded poly(ε-caprolactone)-poly(ethylene glycol)-poly(ε-caprolactone) nanofibers and their *in vitro* antitumor activity against Glioma 9L cells *Nanoscale.* **3** 3825
[103] Sharjeel A, Tanveer H, Zulfiqar A R and Ahsan N 2019 Current applications of electrospun polymeric nanofibers in cancer therapy *Materials Science and Engineering* C **97** 966–77